1. Publication Nº	2. Version	3. Date	5. Distribution
INPE-2317-PRE/076		Feb., 1982	☐ Internal ☒ External ☐ Restricted

4. Origin	Program
DME	PNTE

6. Key words - selected by the author(s)

NUMERICAL WEATHER PREDICTION

7. U.D.C.: 551.509(81)

8. Title

INPE-2317-PRE/076

A 2 1/2 DIMENSIONAL MODEL FOR NUMERICAL WEATHER PREDICTION OVER BRAZIL

10. Nº of pages: 56

11. Last page: 45

12. Revised by

Antonio Divino Moura

13. Authorized by

Nelson de Jesus Parada
Director

9. Authorship Chandrakanta M. Dixit
Wolodymir Boruszewski

Responsible author Wolodymir Boruszewski

14. Abstract/Notes

A 2 1/2 Dimensional Model for Numerical Weather Prediction over Brazil, taking the data paucity into account is described and compared to a quasi-geostrophic model in the advantages it offers. The model accepts as input winds at 2 levels (300 mb and 700 mb) together with boundary-values of the geopotentials at the same levels over a limited area. It proceeds to give a short-range forecast for the winds (including the divergent components) at 300 and 700 mb together with the vertical velocity field at the 500 mb level. Two case (one with 3 consecutive days of data and the other with 2 consecutive days of data) were integrated to test the functioning of the model. The results of the 24 h and 48 h forecast comparison, both from the synoptic point of view and from a numerical point of view, are presented at the end of the work together with figures giving the forecast stream-functions.

15. Remarks

This work was presented in the "I Congresso Brasileiro de Meteorologia", Campina Grande, September 1980.

RESUMO

Um modelo de 2 $\frac{1}{2}$ dimensões para previsão numérica de tempo no Brasil, levando em conta a escassez de dados, é descrito e comparado a um modelo quasi-geostrófico. O modelo recebe como entrada, direção e velocidade do vento em dois níveis (300 mb e 700 mb) juntamente com os valores do geopotencial nos mesmos níveis mas apenas em pontos do contorno. A saída consiste numa previsão de curto prazo para os ventos (incluindo a componente divergente) em 300 mb e 700 mb, bem como a velocidade vertical no nível de 500 mb. Dois casos (um com três dias consecutivos e outro com dois dias consecutivos de dados) foram integrados para testar o funcionamento do modelo. Os resultados das comparações das previsões de 24 h e de 48 h, tanto do ponto de vista sinóptico quanto do numérico, são apresentados no fim do trabalho junto das figuras que fornecem as funções de corrente previstas.

ACKNOWLEDGEMENTS

The authors express their heartfelt thanks to Dr. Luiz Gylvan Meira Filho for his encouragment of the work during its progress and to Dr. Nelson de Jesus Parada, Director - INPE, for his general help.

The authors thanks Mr. Marco Antonio Maringolo Lemes and Dr. Antonio Divino Moura for going through the manuscript and Sra. Sueli Aparecida Freire Valentim Camargo Pinto for her careful typing.

This work was partially financed by FINEP under Convênio FINEP/CNPq 828/79/002 Modelagem Atmosférica.

CONTENTS

LIST OF FIGURES

LIST OF TABLES

1. INTRODUCTION

This report describes a baroclinic model to be used in short-term numerical forecasting. The model was intentionally designed to be as simple as possible due to the existing computational facilities; nevertheless its computer program is amenable to accept future modifications and more sophistications. The first part of the report gives some information regarding the theory behind the model, together with all simplifying assumptions. The second part deals with a brief description of certain practical aspects and with some features which require a few special subroutines for their adaptation into the model.

The general objective was to obtain a model which could give a 24 hour forecast in about 1 hour of computer time when the input is already available in some gridded form. The part pertaining to objective analysis, i.e., the step which converts the input data at observational points into a set of data at a desired uniformly spaced grid is not dealt with.

Keeping the presentation to its briefest limits, the barotropic counterpart of the model is described. Its consists of the integration of:

$$\frac{d\eta}{dt} = 0$$

where

$$\eta = f + \frac{1}{a \cos\phi} \left(\frac{\partial v}{\partial \lambda} - \frac{\partial}{\partial \phi} (u \cos\phi) \right) \qquad (1)$$

and

$$\frac{d}{dt} = \frac{\partial}{\partial t} + V_\psi \cdot \nabla \qquad (2)$$

with the customary termilonogy and omission of the other terms. The point of using Equation (1) is that as Neamtan (1946) has shown, it admits finite amplitude exact solutions and thus permits a verification of the

program. The advantage over using quasi-geostrophy is that the limitations of constant f_o are not imposed and thus the region of forecast can include even the equator. In the test of the program a theoretical Neamtan wave was allowed in a region extending from 40^oS to 40^oN. Other tests were also made with real data including equatorial regions. These results are not presented in this report since they will be included in another report to be shortly submitted.

Though the model has 3 levels, it resembles the first version of a 3 level model: 2 for application of the vorticity equation and an intermediate one for application of the thermodynamic equation.

The similarity lies in the fact that at the intermediate level the equation for the vertical velocity (ω) is solved. This model was baptized by Eady as 2 1/2 dimensions [Eady (1952), Ogura (1957)]. The idea in mentioning the third dimension (z or p) as incomplete is that it is very grossly represented by the finite difference spacing in the z or p direction, while the horizontal (x and y) directions are generally covered by a system of grid-points which lead to no effective loss of dimensionality. Also the thermodynamic equation is applied to "sandwitched" levels, leading to an incompleteness of information. Though the name is not appropriate to the type of model here described, the authors still prefer the former one because it emphasizes the fact that the vertical dimension (z or p) is grossly represented.

The simplest baroclinic representation is of the type described by the quasi-geostrophic model. This model has 3 levels, with the middle (LM) at 500 mb - close to the supposed level of nondivergence. This fact allows for a considerable oversimplification of the model. The information levels are L_1, L_M and L_3, (Figure 1) where the vorticity equation can be applied in principle.

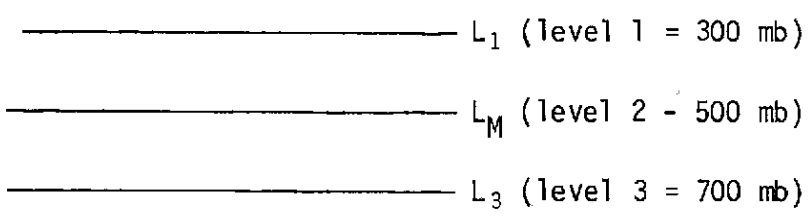

Fig. 1 - The layout for a quasi-geostrophic model.

L_1 and L_M have the same difference Δp (of pressure) as L_M and L_3. This is not a theoretical necessity, but only of computational convenience.

The appropriate system of equations of the model is

$$\frac{\partial \eta_3}{\partial t} + V_3 \cdot \nabla \eta_3 = f_o \frac{\omega_2}{\Delta p} \tag{3}$$

$$\frac{\partial \eta_1}{\partial t} + V_1 \cdot \nabla \eta_1 = - f_o \frac{\omega_2}{\Delta p} \tag{4}$$

where

f_o is a representative Coriolis parameter, constant to ensure the integral constraint on energy, V_1 - two-dimensional horizontal wind vector at level 1, V_3 - two-dimensional horizontal wind vector at level 3, η_1 - vertical component of absolute vorticity at level 1, η_3 - vertical component of absolute vorticity at level 3, ω_2 - vertical velocity at level L_M.

The application of the thermodynamic equation at the middle level furnishes a third equation under the hypothesis that the static stability $\sigma = \frac{-1}{\Theta} \frac{\partial \Theta}{\partial p}$ is a constant. Within the limitations of the model proposed, these restrictions (σ constant; f_o constant) were necessary. However, the application of the thermodynamic equation is effectively equivalent to a kind of oversimplified ω equation. Within the quasi-geostrophic hypothesis, the advective terms in equation 1 and 2 ($V_1 \cdot \nabla_{\eta_1}$ and $V_3 \cdot \nabla_{\eta_3}$) were evaluated using the geostrophic wind and the vorticity replaced by its geostrophic value:

$$fu_g = - \frac{\partial \Phi}{\partial y} \; ; \qquad fv_g = \frac{\partial \Phi}{\partial x} \tag{5}$$

where Φ is the geopotential.

This is essentially the basic philosophy of the quasi-geostrophic 2 1/2 dimensional model. In applying this model to the South American region, the principal difficulty lies in the fact that the region of interest covers quite a stretch of the equatorial belt.

The authors feel that a map extending from 10^{o}N to perhaps 35^{o}S is necessary to achieve a representative picture of the wind flow over the region. Even few observations in the North Hemispheric region (0^{o} to 10^{o}N) appears to be necessary to make any reliable analysis on a daily basis if the paucity of data in this huge latitudinal extent is considered. Though of course a suitable choice of f_o could avoid many problems, the known failure of geostrophic relation in the equatorial belt would call for a model which would rather avoid the geostrophic wind and geostrophic vorticity.

2. THE MODEL

2.1 - GENERAL CONSIDERATIONS

In searching for a model applicable to the Brazilian region, one had to look for a model which was as simple as possible and yet could have a possibility of being transformed into an eventual multi-level (> 3) model. Naturally a first choice was a 2 1/2 dimensional model which did not use geostrophy (this choice was also partially controlled by the limitations of the then existing computer facilities). One iterative alternative (Kubota, 1960) was very satisfactory from the mathematical point of view but too time consuming (even for executing a few time steps of 10 minutes it requires more than 3 hours) and had to be given up, because of the operational aspect involved.

The final choice was made after a few trials regarding the feasibility, being decided upon by responding to the following:

1. When operational, will the model give a 24 hour prediction say in 40 minutes of computer time?
2. Is the model simple enough?
3. Can it be extended to a multi-level model?
4. Can it be made to include some of the physics not included in the oversimplified versions?
5. Does it furnish vertical velocities?

In addition, it has also to be remembered that the simplified baroclinic model must yet allow investigations of oversimplified diagnostic problems - like, for instance, instability investigations, etc.

2.2 - GENERAL DESCRIPTION

The model finally chosen was adapted after also considering the data situation in Brazil.

The simplest consistent system consists of applying the vorticity equation at levels 1 and 3 in the form.

$$\frac{\partial \zeta}{\partial t} + V_\psi \cdot \nabla\zeta + (V_\psi + V_\chi) \cdot \nabla f = f \frac{\partial \omega}{\partial p} \tag{6}$$

and the linear balance equation, i.e.,

$$\nabla \cdot (f\nabla\psi) = \nabla^2\Phi \tag{7}$$

where

V_ψ : rotational part of the horizontal wind vector;

V_χ : divergent part of the horizontal wind vector.

This removes the necessity of holding f constant as in the quasi-geostrophic models. The ψ functions at levels 1 and 3 are determined in terms of wind data by a method described by Rosenthal and Hawkins (1975).

The corresponding ω equation is:

$$\nabla^2 (\sigma\omega) + f^2 \frac{\partial^2\omega}{\partial p^2} = R \tag{8}$$

where σ is held as a constant and

$$R = f \frac{\partial}{\partial p} \left[\underset{\sim}{V}_{\psi} . \nabla (\zeta + f) \right] - \nabla^2 \left[\underset{\sim}{V} . \nabla \left(\frac{\partial \Phi}{\partial p} \right) \right] + f \nabla f . \frac{\partial \chi}{\partial p} - \nabla f . \nabla \frac{\partial^2 \psi}{\partial p \, \partial t} \qquad (9)$$

As contrast to the quasi-geostrophic formulation, this has the disadvantage of having more terms on the right-hand side. Apart from the terms containing the Laplacian of thermal advection and the differential advection of vorticity, it requires an evaluation of the χ field (corresponding to the divergent-component of the wind) and also of a term which involves a time derivative. However weighed against the possible disavantages of a constant f_o - which in quasi-geostrophic models is forced to be constant due to energetic consistency conditions- the additional work involved in the evaluation of the above mentioned terms seems to be worthwhile to have a better ω field than is given by ω resulting from the quasi-geostrophic assumptions.

This may be simply explained as follows. The vorticity equation at level 1 may be written as

$$\frac{\partial \zeta}{\partial t} + \underset{\sim}{V}_1 . \nabla \eta = - f \left(\frac{\partial \omega}{\partial p} \right)_1 \qquad (10)$$

or

$$\frac{D\eta_1}{D_t} = F_1 = - f \left(\frac{\partial \omega}{\partial p} \right)_1 = - f_o \left(\frac{\partial \omega}{\partial p} \right)_1 + (f_o - f) \left(\frac{\partial \omega}{\partial p} \right)_1 \qquad (11)$$

This may be interpreted as saying that F_1 is a "source-term" for η_1.

In a quasi-geostrophic system where f_o replaces f, the regions where $|f| < |f_o|$ receive an unnecessary overweightage $\frac{|f_o|}{|f|}$.

Further, the ω equation in the quasi-geostrophic system also has to use f_o. This results in a multiplication of $\frac{\partial^2 \omega}{\partial p^2}$ by $\left(\frac{f_o}{f} \right)^2$.

in regions where $|f| < |f_o|$.

Within the limitations of the system of equations and the hypotheses made, one may regard the physics of the model as being well represented by the various terms concerned. The effects of the factor $\frac{f_o}{f}$, both in the ω equation directly and in the vorticity equation indirectly, are likely to create distortions in the quasi-geostrophic system. For this reason the system,finally adopted,used the ω equation in the form of equation (8).

2.3 - THE EQUATIONS OF THE MODEL

The model actually designed is also schematically represented in Figure 2.

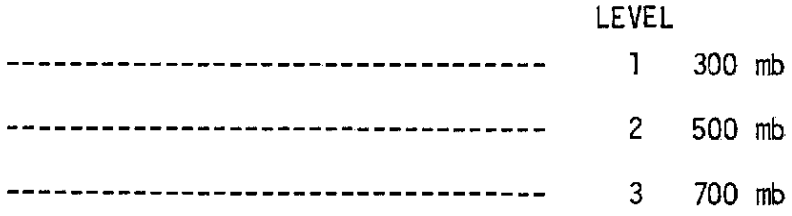

Fig. 2 - The layout of the model.

The equations of this model are:

$$\frac{\partial \zeta_1}{\partial t} + V_{\psi_1} \cdot \nabla \zeta_1 + (V_\psi + V_\chi)_1 \cdot \nabla f = f \left(\frac{\partial \omega}{\partial p} \right) \tag{12}$$

$$\frac{\partial \zeta_3}{\partial t} + V_{\psi_3} \cdot \nabla \zeta_3 + (V_\psi + V_\chi)_3 \cdot \nabla f = f \left(\frac{\partial \omega}{\partial p} \right)_3 \tag{13}$$

$$\nabla \cdot (f \nabla \psi) = \nabla^2 \phi, \text{ at levels 1 and 3} \tag{14}$$

$$\nabla^2 (\sigma \omega) = R - f^2 \frac{\partial^2 \omega}{\partial p^2} \tag{15}$$

$$\psi_2 = \frac{\psi_1 + \psi_3}{2} \tag{16}$$

In the first trials some easily discardable oversimplifications were made - although the program includes all the terms of the equations written above.

2.4 - SOME DETAILS REGARDING GRID AND DATA

The levels selected were such that the level 2 was quite close to the so-called level of nondivergence (500 mb) and $p_2 - p_1 = p_3 - p_2$.

The input data consist of winds at levels 1 and 3 together with boundary values of the geopotentials. In practice the data included the wind and geopotentials at level 2, but this was used merely to facilitate some diagnostic studies.

These data were picked up over a grid with a spacing of 2.5 degrees in latitude and longitude. The program as written does not, however, require the latitude spacing to be the same as the longitude spacing.

The region covered extends from

$40^{o}W$	to	$75^{o}W$
$35^{o}S$	to	$10^{o}N$

and has 19 x 15 grid-points.

With the wind data at levels 1 and 3, ψ_1 and ψ_3 fields were obtained by using one of the methods suggested by Rosenthal and Hawkins (1965) (see, also Santos and Dixit, 1977) and ψ_2 was put as $\frac{\psi_1 + \psi_3}{2}$. With the linear balance equation and the boundary values of the geopotentials at levels 1, 2 and 3 the geopotentials at level 1, 2 and 3 (Φ_1, Φ_2, Φ_3), in the interior of the grid were computed. Preferring to work with the C. G. S. system and using the heights in cm, the Φ fields were converted to the geometric heights by using.

$$Z = \frac{R\Phi}{\left(\frac{Rg_\phi}{9,8} - \Phi\right)} \qquad (17)$$

where

$R = \frac{2g_\phi}{-\left(\frac{\partial g}{\partial z}\right)_{z=0}}$ is a function of latitude (Smithsonian Tables, 1949).

3. FINITE DIFFERENCING SCHEMES AND INTEGRATION

3.1 - SOME REMARKS ON THE FINITE DIFFERENCING SCHEMES

Throughout the program, central differencing schemes were utilized for space derivatives. The Laplacian $\nabla^2\psi$ was replaced by Figure 3:

$$\alpha_1\psi_1 + \alpha_2\psi_2 + \alpha_2\psi_3 + \alpha_4\psi_4 + \alpha_9\psi_9$$

where

$$\alpha_1\ \alpha_3 = \frac{1}{a^2\cos^2\phi} \quad \frac{1}{(\Delta\lambda)^2} \qquad \alpha_2 = \frac{1}{a^2(\Delta\phi)^2}\left[1 - \frac{\tan\phi}{2\Delta\phi}\right]$$

$$\alpha_9 = \frac{1}{} + \frac{1}{a^2 2\Delta\phi} \qquad \alpha_4 = \frac{1}{a^2(\Delta\phi)^2}\left[1 + \frac{\tan\phi}{2\Delta\phi}\right]$$

in accordance with the spherical coordinates definition of $\nabla^2\psi$. The coefficients in the relaxations hence were latitude dependent.

The advection terms could be evaluated by the customary evaluation of the spherical Jacobian (Kubota, 1960) defined by

$$J_{\phi\lambda}(u,v) = \frac{1}{a^2\cos\phi}\left[\frac{\partial u}{\partial\phi}\cdot\frac{\partial v}{\partial\lambda} - \frac{\partial u}{\partial\lambda}\cdot\frac{\partial v}{\partial\phi}\right]$$

The vorticity and divergence also included the u and v terms.

$$\eta = f + \frac{1}{a \cos\phi} \left[\frac{\partial v}{\partial \lambda} - \frac{\partial}{\partial \phi} (u \cos\phi) \right] \tag{18}$$

$$D = \frac{1}{a \cos\phi} \left[\frac{\partial u}{\partial \lambda} + \frac{\partial}{\partial \phi} (v \cos\phi) \right]$$

These quantities were evaluated at (I,J) points by computing each of the brackets like $u \cos\phi$ and $v \cos\phi$ as separate functions. Thus in η the finite centred difference was for $(u \cos\phi)_{\phi+\Delta\phi}$ - $(u \cos\phi)_{\phi-\Delta\phi}$.

3.2 - THE TIME-INTEGRATION SCHEME

The marching process was started by integration of equations of the type $\nabla^2(\frac{\partial \psi}{\partial t}) = a$, giving $\frac{\partial \psi}{\partial t}$ through inversion of the Laplacian. The first step in time was done with the predictor-corrector of Euler modified method.

If a subscript denotes time, this amounts to solving

$$\frac{dy}{dt} = f(y,t) \tag{19}$$

by setting

$$y^*_{i+1} = y_i + \Delta t \left[f(y_i, t) \right] \tag{20}$$

as an intermediate variable, computing

$$f^* = f (y^*_{i+1}, t) \tag{21}$$

and then setting

$$y_{i+1} = y_i + \Delta t \left[f (y_i, t) + f^* \right] \tag{22}$$

where

i, i+1 denote y at $t = i\Delta t$ and y at $t = (i+1)\,\Delta t$

Of course this is a low order Runge-Kutta method. The method was selected after trying a few other methods. A higher order Runge-Kutta method is more accurate but quite time consuming. Since FSTEP (the subroutine which just advances data by one time step) is used quite a number of times, the economy is worthwhile.

After FSTEP the remaining time steps in a sequence completing a 6 hours cycle were taken by a subroutine STEP, which is essentially a leapfrog scheme with simulated backward differences applied to the standard 3 time levels. Essentially,the scheme consists of solving

$\frac{d\psi}{dt} = F$; knowing ψ_i and ψ_{i-1} by the following scheme:

$$\psi^* = \psi_{i-1} + 2.0\ \Delta t\ (F_{i-1}) \tag{23}$$

$$\psi_{i+1} = \psi_i + \Delta t\ \left[\ F(\psi^*)\ \right] \tag{24}$$

3.3 - SMOOTHING

A smoothing process was applied every 6 hours to the ψ and Φ fields at all the levels to remove waves of wavelengths less than 3 grid-points. If smoothing was applied more frequently it would continually act as a sink of energy. For integration of long periods (more than 6 hours) the scheme consisted of

FSSSS (smooth) FSSSS (smooth) FSSSS ...

where

F: One time step t to t+1

S: Three time level leapfrog t-1, t to t+1

F generated consistent fields ψ (t) and ψ (t-1) which could then be operated upon by the S subroutine. Such a mixture of leapfrog and one

time step method is recommended by Arakawa and Lamb (1977), when the process was simply

FSSSSSSS with smoothing every 6 hours,

the results were not as good as with the above mixture and also the second scheme tended to blow-up after about 4 days if S were not also the Matsuno type.

A possible computational alternative is to smooth the fields at t = i and t = i - 1 and continue with the leapfrog. But ψ_i is not a forecast of ψ_{i-1} after a time due to nonlinearities and the smoothing process may be regard simply as a filter. Thus it becomes necessary to reintroduce, after smoothing, a new time step to obtain consistent fields.

3.4 - HEUN'S METHOD

$$\frac{d\psi}{dt} = F$$

$$\psi(t+1) = \psi(t-1) + \frac{\Delta t}{3}\left(F(t+1) + 4F(t) + F(t-1)\right) \qquad (25)$$

The computational being iterative, i.e., F is known at t and t - 1 and a first guess at F(t + 1) is made, after obtaining $(\frac{\partial\psi}{\partial t})_{t+1}$ by the inversion of $\nabla^2(\frac{\partial\psi}{\partial t})$. This fed again into equation (25). Usually an "ideal" end to the iteration is: $\psi(t+1)$ differs from its previous estimate by less than 1% on all points of the 15 x 19 grid. This took a long time and required something like 4 to 5 iterations. However, even a single iteration produces a sufficiently acceptable result. Since the purpose of the present work was to have a method for short time prediction within a resonable computer time, Heun's method was abandoned. For some future work however, the program as written, still contains segments pertaining to his method.

3.5 - THE VERTICAL VELOCITY COMPUTATION

The vertical velocity was assumed to be of the form $\omega=k(x,y)p(p-p_0)$

In the relaxations for the ψ and Φ fields, the boundary conditions utilized were first to keep the older values on the boundary. After relaxation, the fields were extrapolated from the interior to the boundary by an 8 point extrapolation trigonometrical formula. This allowed for a change in the boundary values. In the initial stages, reiteration was performed with the new values for consistency but this was not found worthwhile.

4 - TEST OF THE PROGRAM WITH RESULTS

The program was tested on two sets of data for which grid-point values of winds and geopotentials were available one for two days, i.e., 9-10 of August, 1971, and the other for 12-13-14 of October, 1971.

It is proposed, with the help of grid-point data available in tapes for analysis of tropical regions, to make a more extensive and comprehensive test which might be considered free from the subjective element in the analysis actually utilized in the two cases used for this text.

In Figures 4, 5 and 6 are presented two cases of 24 hours integration and 48 hours integration.

As, in both cases, the situations were those of inclined anticyclones, they are described in terms of 500 mb only(Figures 4 (B), 4 (E), 4 (H) in the first case; Figures 5 (B), 5 (E), 5 (H), 6 (B), 6 (E) in the second case).

The comparisons with the observed values have been made in two ways:

I) Comparing the synoptic patterns;

II) By computing the following numbers:

II.1) Root mean square error in the zonal component of the wind, latitude by latitude;

II.2) Root mean square error in the meridional component of the

the point $10^{o}S/58^{o}E$.

Twenty-four hours later, the ridge shows little movement in its western part, but the eastern part seems to have suffered a large southward displacement to about $18^{o}S$.

At t = 48 hours, the ridge, as a whole, seems to have moved northwards to about $5^{o}S$ with an antycyclone centre at $57^{o}W$.

In the 24 hours forecast, the ridge is shown at $11^{o}S$ with a very weak centre.

In the 48 hours forecast, the ridge moves northwards, but is still at about $9^{o}S$.

In the case during the 48 hours, there was a large oscillation of the ridge, at least at its eastern end. Unless, if this is a result of the faulty analyses due to paucity of data, which is quite possible, this oscillation was not reproduced on the forecast.

In making the comparisons it may be noted that:

1) There is a large element of subjectivity in the analysis at various levels, leading to errors in directions and in speeds of winds;

2) There are regions of information gaps of which three important ones, related to the numerical comparison made later, are:

   2.1) the latitude $5^{o}S$ has a large stretch of no information;

   2.2) $65^{o}W$ has very few observations though it runs over land;

   2.3) $40^{o}W$ has a large stretch over the oceans.

Particularly over all the areas in vicinity of localities mentioned in 2.1, 2.2 and 2.3 above, the analysis may be considered to have more error than over other regions.

Trough the correlation coefficients of the forecast

with zeros of ω at $p = 0$, and $p = p_o$, which was taken to be at 1000 mb. Applying this at 500 mb results in a Helmholtz equation for $k(x,y)$ given by

$$\Delta^2 k + \mu k = \delta$$

where

$$\mu = 2f^2/Q \quad ; \; Q = \sigma p_M (p_M - p_o) \quad ; \; p_M = 500 \text{ mb} \tag{26}$$

$$\delta = R_1/Q \quad ; \; R_1 = f \frac{\partial}{\partial p} \left[V_\psi . \nabla (\zeta + f) \right] - \nabla^2 (V . \nabla \frac{\partial \phi}{\partial p}) + \nabla f . \frac{\partial \chi}{\partial p} \tag{27}$$

The boundary condition $\omega = 0$ was utilized. The condition that $\omega = 0$ at $p = p_o$ can be dropped later to include the Ekman layer top velocity at p_o. In solving the ω equation numerically, the time dependent term in δ was dropped as it was found to be too small. The relaxation was actually done by the same relaxation program which inverts poissonians but by adjusting in time the latitude dependent coefficients in $\sum_{j=1}^{9} \alpha_j \psi_j = 0$, with indexes as in the figure below:

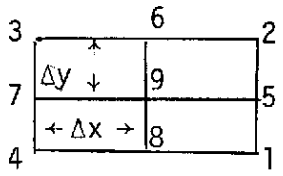

Fig. 3 - Single indexing scheme normally used for evaluation of $\nabla^2\psi$.

Extrapolation of vertical velocities to other levels is possible, but is not justifiable in view of the oversimplifications of the model.

With the equation for ω, $\frac{\partial \omega}{\partial p} = 2kp - kp_o = - \nabla . V$, the divergence at levels 1 and 3 is obtained via $k(x,y)$ by simply solving $\nabla^2 \chi = \frac{\partial \omega}{\partial p}$ (in this simplified model, $\chi_1 = - \chi_3$, $Div_1 = - Div_3$, $Div_2 = 0,0$). For obtaining the divergent component of the wind, the boundary condition was simply $\chi = 0$. The output contains the vector sum of the divergent and nondivergent components as well as a graphic representation of the ψ field. (28)

wind, latitude by latitude;

II.3) Correlation coefficients between observed and predicted zonal winds for each meridian;

II.4) Correlation coefficients between the observed and predicted meridional components for each latitude.

The idea in making the zonal wind (observed versus predicted) comparisons only meridion wise was to see how well prediction had caught the North-South motion movement of the systems (if any), same applying to the comparison latitude wise of the meridional component v with respect to east-west motion of systems (if any). The authors are aware of more sophisticated methods of comparison, but did not use the technique in view of the small number of occasions available.

The numerical results are given in Tables 1, 2 and 3 at 10^{o} intervals, though they were computed for 2.5^{o} intervals.

Case 1: (9.8.71 1200 GMT t=0)

At t = 0 anticyclone was centred at $23^{o}S/50^{o}W$ with a ridge running approximately along $23^{o}S$. There is a noticeable trough oriented SW-NE from $10^{o}S/60^{o}W$ and running northeastwards.

Twenty-four hours later, the patterns seem to have moved northwards, with the ridge location at about $17^{o}S$. There is a trough corresponding to the trough at t = 0, but it is much weaker and runs NS. The sharply marked centre at t = 0 was given place to a diffused central region. In the forecast for 24 hours an anticyclone centre is still forecast at $17^{o}S/58^{o}E$, and a ridge runs along $17^{o}S$. Though there is no noticeable trough in the wind field, the vorticity field shows a corresponding structure. The northward shift of the ridge has been correctly anticipated by the forecast.

Case 2 (12/10/71 t = 0 h)

At t = 0, we have a ridge at approximately $12^{o}S$, with an anticyclone centre at $62^{o}E$. There exists a weak trough running NE through

components of the winds against the observed components were obtained on a 2.5^{o} latitude/longitude grid, only a brief summary is reproduced in Tables 1 to 3.

The numbers in the tables show, in general, fairly large and acceptable correlation coefficients (some exceeding .95). It must be remarked, however, that a few of the correlation coefficients were negative, though very small.

Of the two types (zonal components compared along meridians and meridional components compared along the latitudes) none seems be better forecast than the other. This is significant in view of the fact that, in general, the meridional components were not as strong as the zonal components.

5. CONCLUDING REMARKS

From the above we might reach an encouraging and tentative conclusion that the method of forecasting is applicable even with the limitation of data and has fair degree of accuracy. It at least merits extension to two more levels so that the orographic effects and the effects of the type of Ekman pumping can be included. Further, it is within the limitations of the present computer at INPE to obtain a 48 hours forecast with about 90 minutes of computing time. An extension to more levels in the next logical step and the results of the present test justify such an extension.

REFERENCES

ARAKAWA, A. and LAMB, V.R. *Computational design of the basic dynamical processes of the UCLA general circulation model.* Methods in Computational Physics, 1977, vol. 17, Academic Press.

EADY, E. *Note on weather computing and the 2 1/2 dimensional model.* Tellus, 4, 1952, 137-167 pp.

KUBOTA, S. *Surface spherical harmonic representation of system of equations for analysis.* Paper in Met. and Tokio, 1960, 145-178 pp.

NEAMTAN, S. M. *On the motion of harmonic waves in the atmosphere.* Journal of Meteorology, 1946, vol. 3, 53-56 pp.

OGURA, Y. *Wave solutions of the vorticity equation for the 2 1/2 dimensional model.* Journal of Meteorology, 1957, vol. 114, 60-69 pp.

ROSENTHAL, L. S. and HAWKINS, H. F. *On the computational of stream functions from the wind field.* Monthly Weather Review, 1965, vol. 93, (4).

SANTOS, R. P. and DIXIT, C. M. *Sobre um método para computar função de corrente nas latitudes tropicais a partir de vento observado.* Work presented at S. B. P. C. 29th Reunião, 1977.

SMITHSONIAN Tables, Ed. by list. R. J. Smithsonian Misc. Collections Smithsonian Institution Press, City of Washington, 1949, 520 pp.

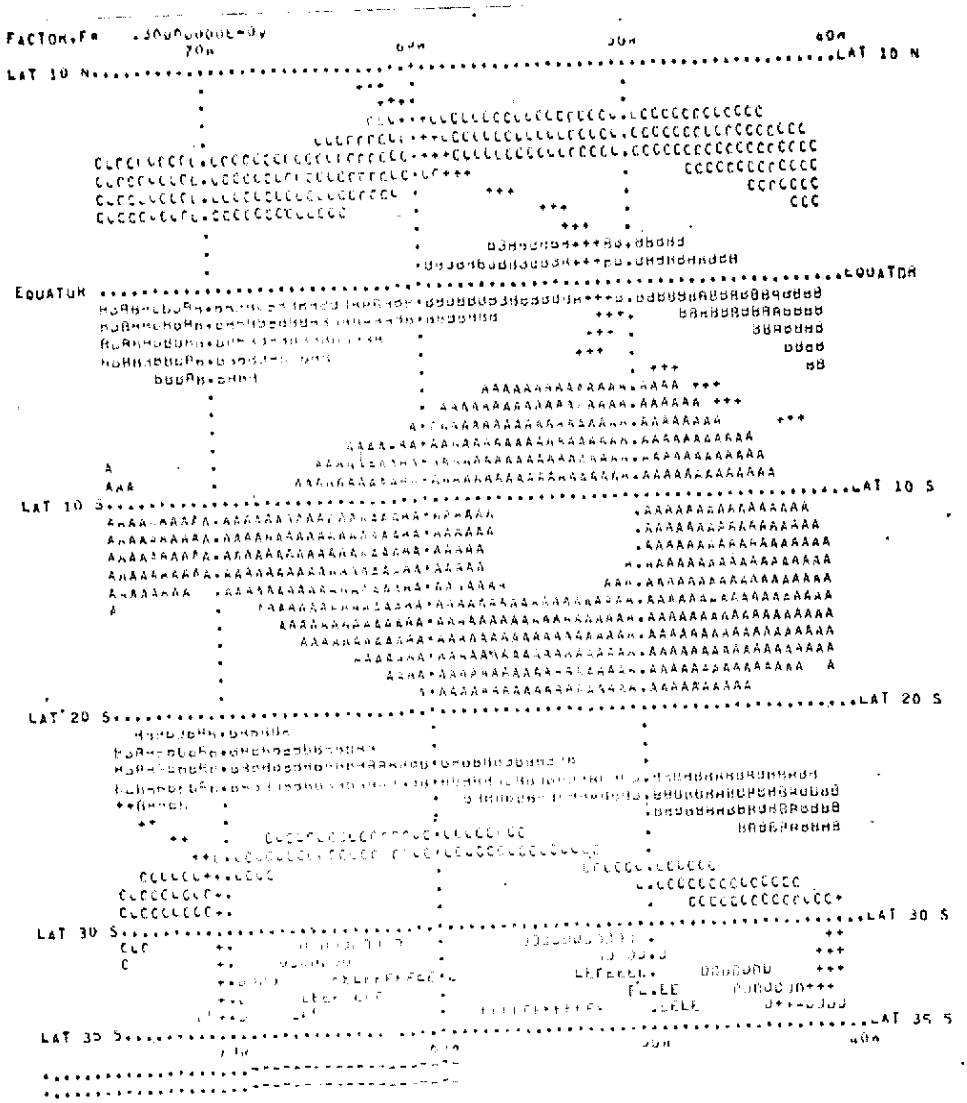

Fig. 4 (A) - ψ for 9/8/71 1200 GMT; 300 mb, observed (t = 0 h)

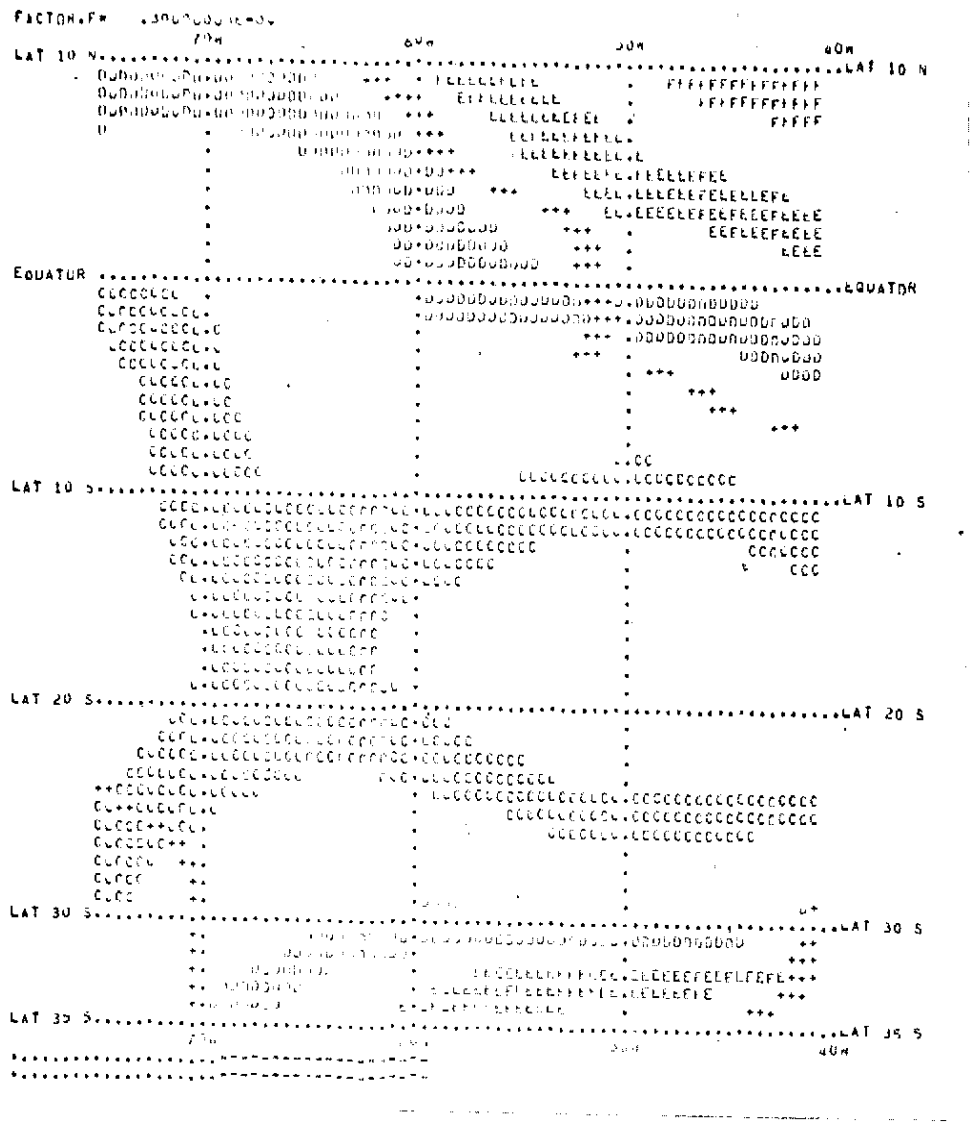

Fig. 4 (B) - ψ for 9/8/71 1200 GMT; 500 mb, observed (t = 0)

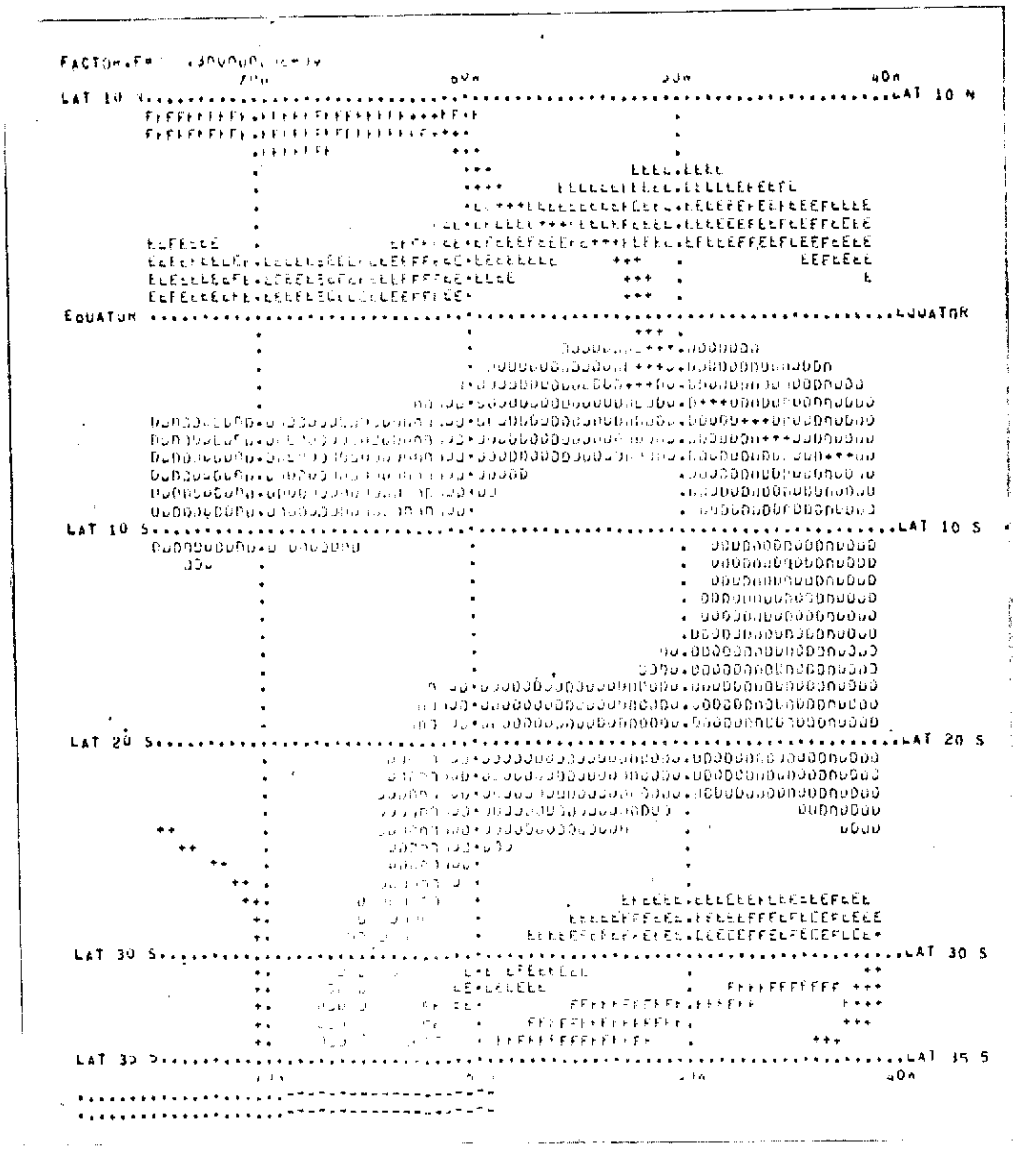

Fig. 4 (C) - ψ for 9/8/71 1200 GMT; 700 mb; observed (t = 0)

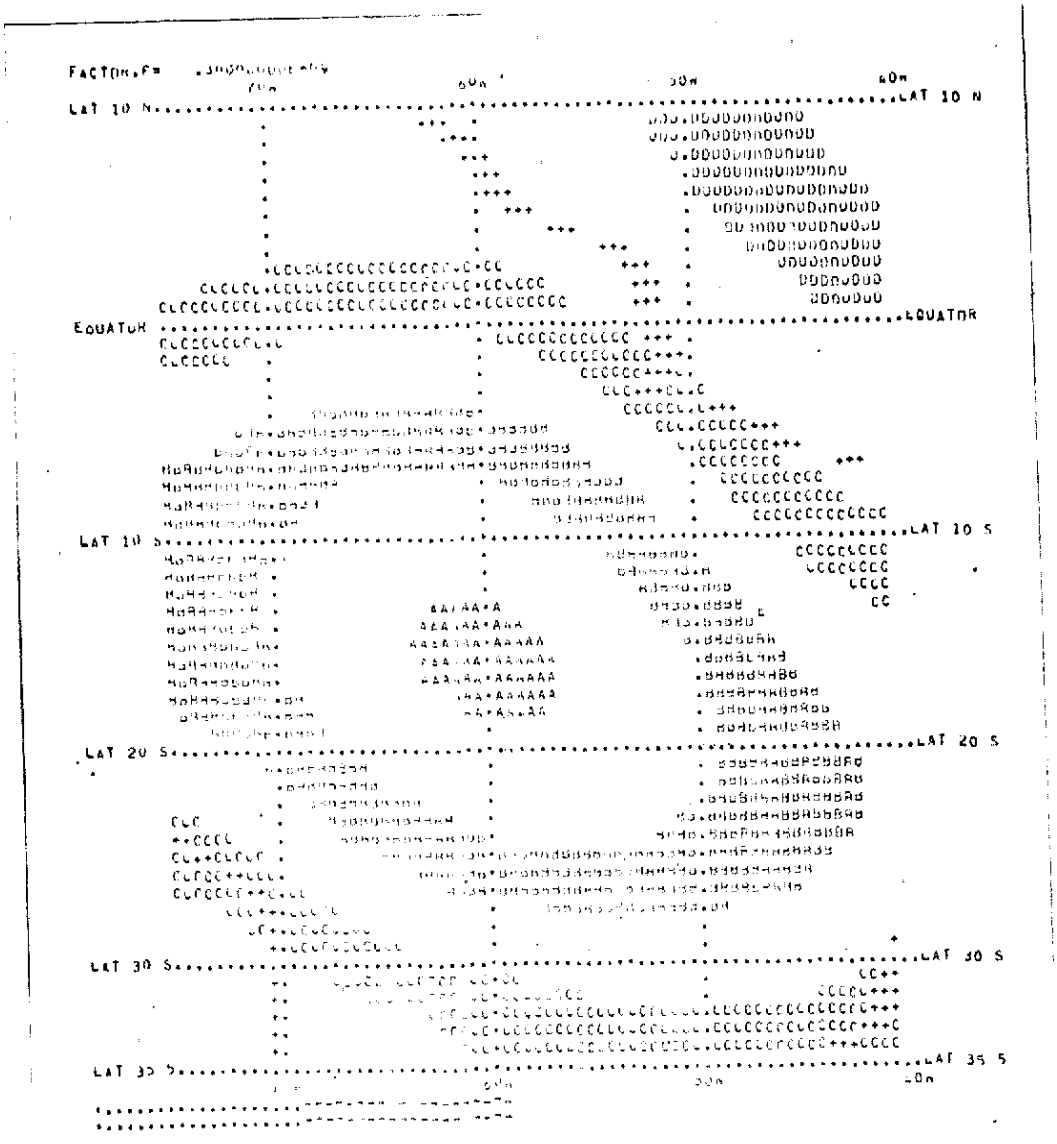

Fig. 4 (D) - Forecast ψ for 10/8/71 1200 GMT; 300 mb (t = 4 h)

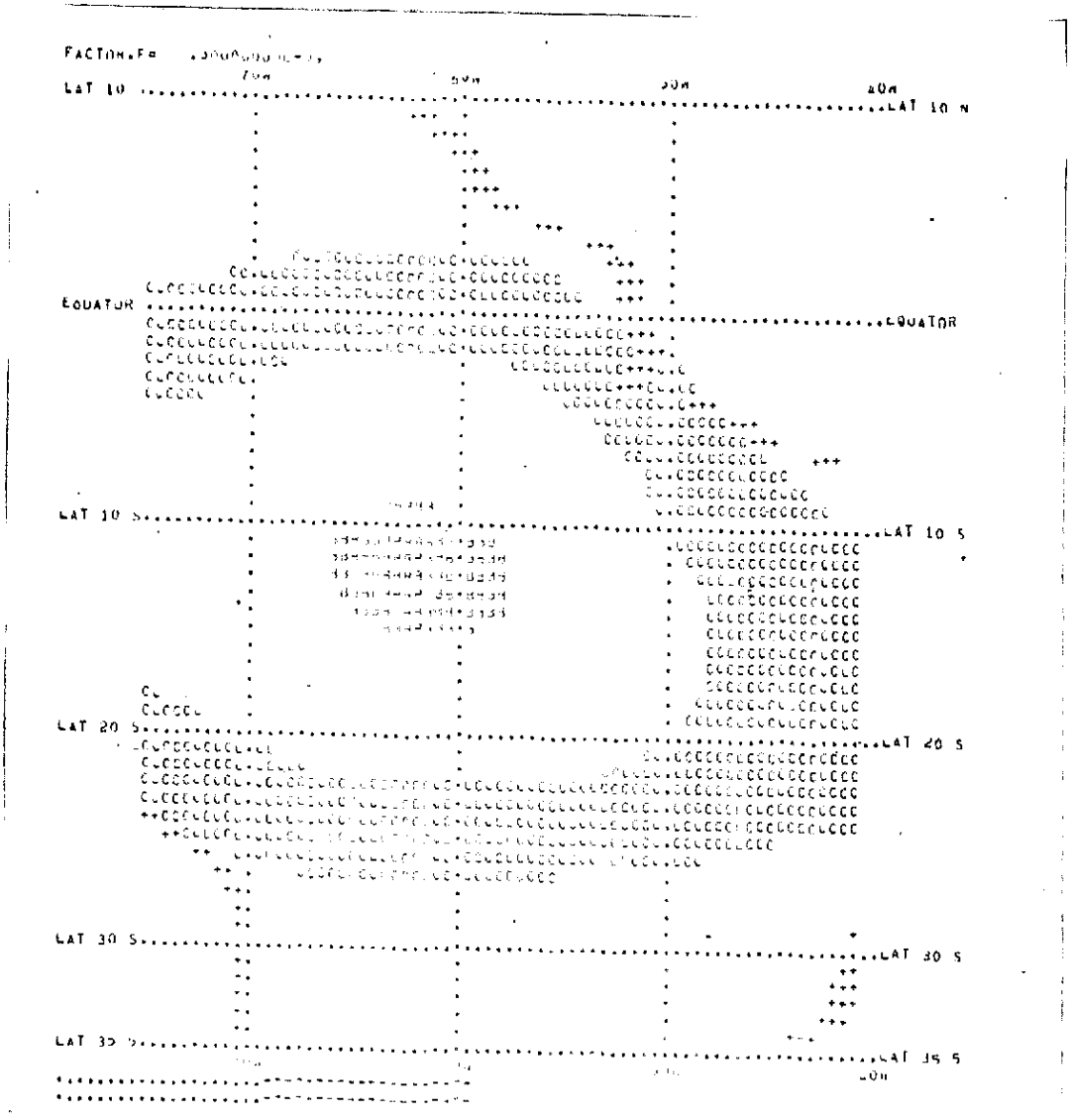

Fig. 4 (E) - Forecast ψ for 10/8/71 1200 GMT; 500 mb (t = 24 h)

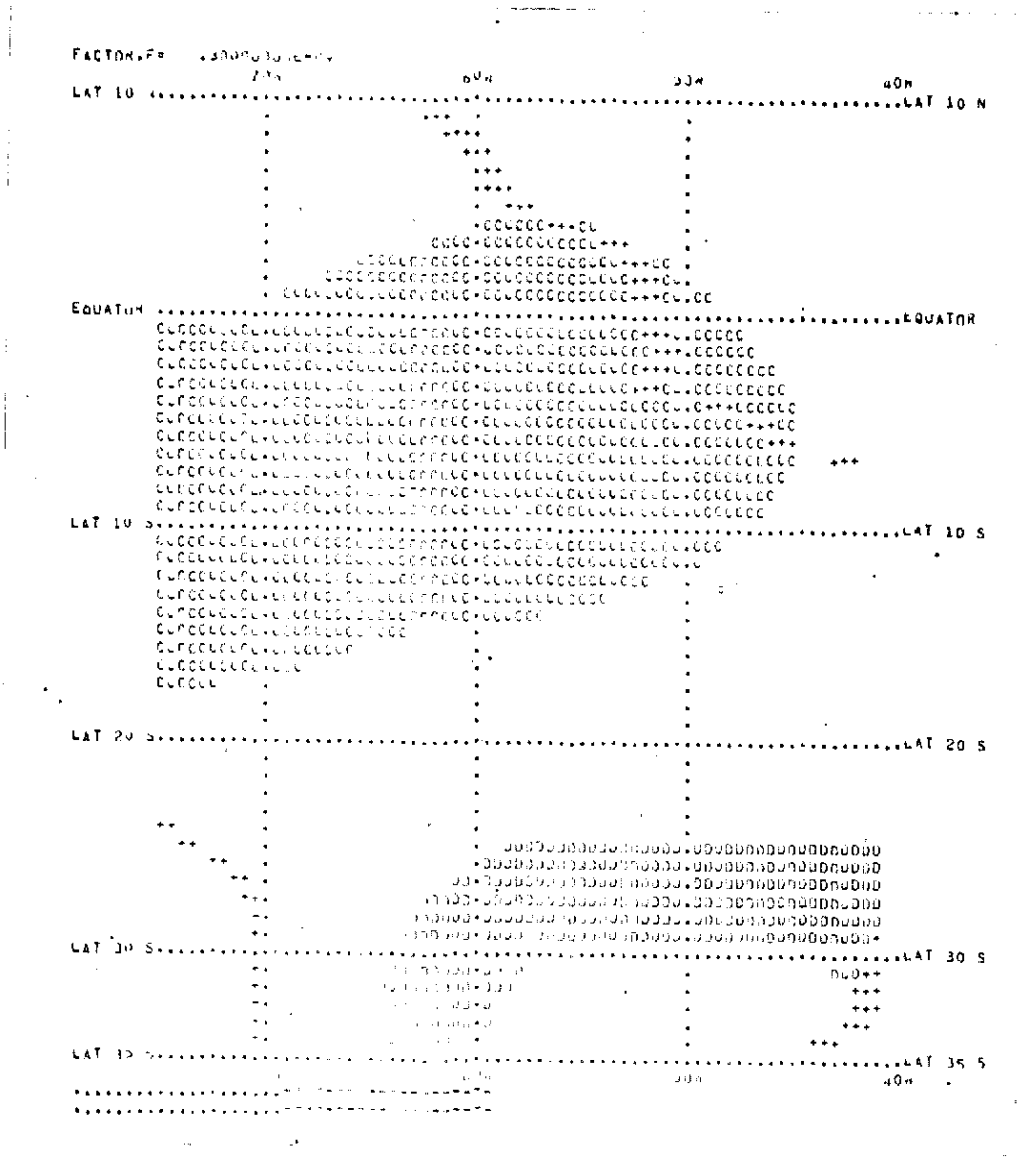

Fig. 4 (F) - Forecast ψ for 10/8/71 1200 GMT; 700 mb (t = 24 h)

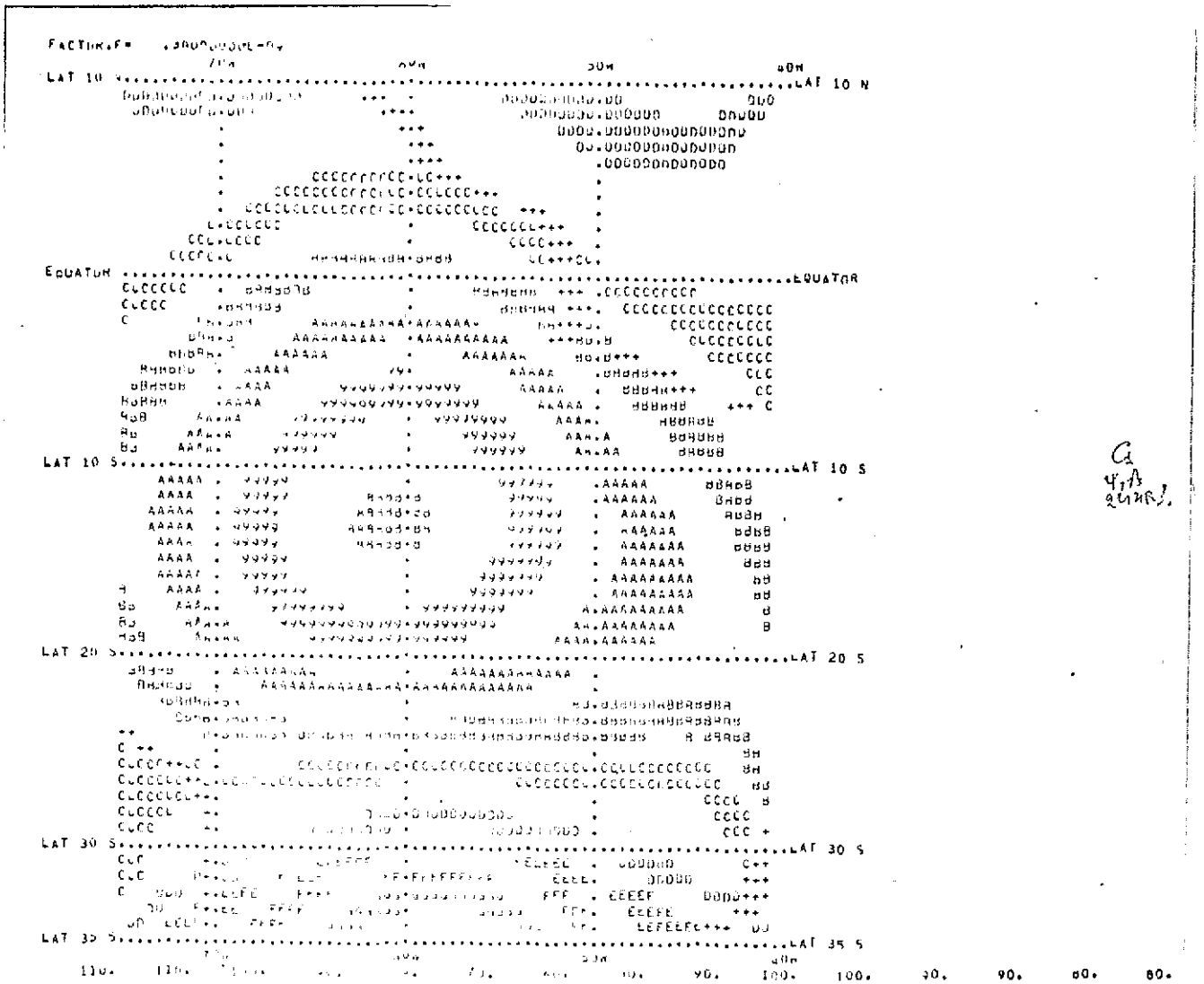

Fig. 4 (G) - (Observed) ψ for 10/8/71 1200 GMT; 300 mb (t = 24 h)

Fig. 4 (H) - (Observed) ψ for 10/8/71 1200 GMT; 500 mb (t = 24 h)

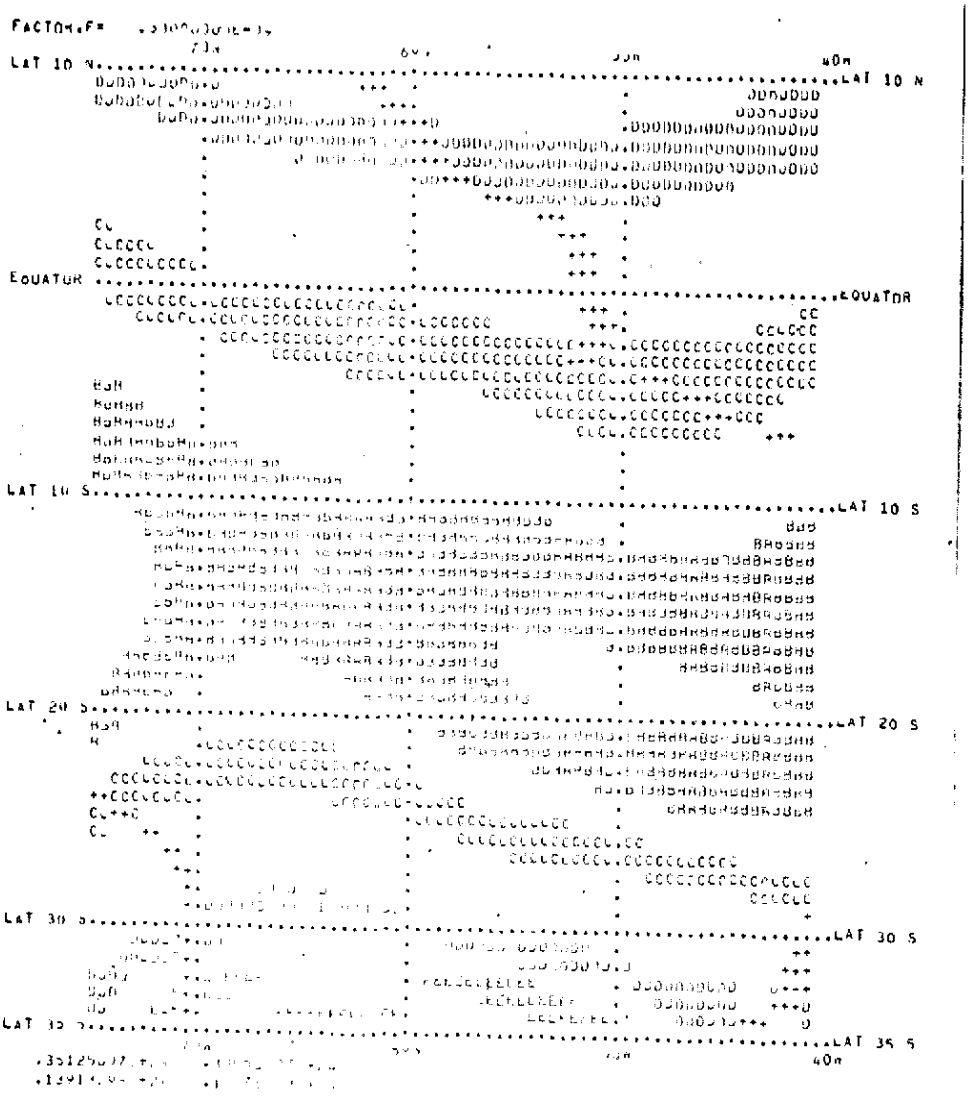

Fig. 4 (I) - (Observed) ψ for 10/08/71 1200 GMT; 700 mb (t = 24 h)

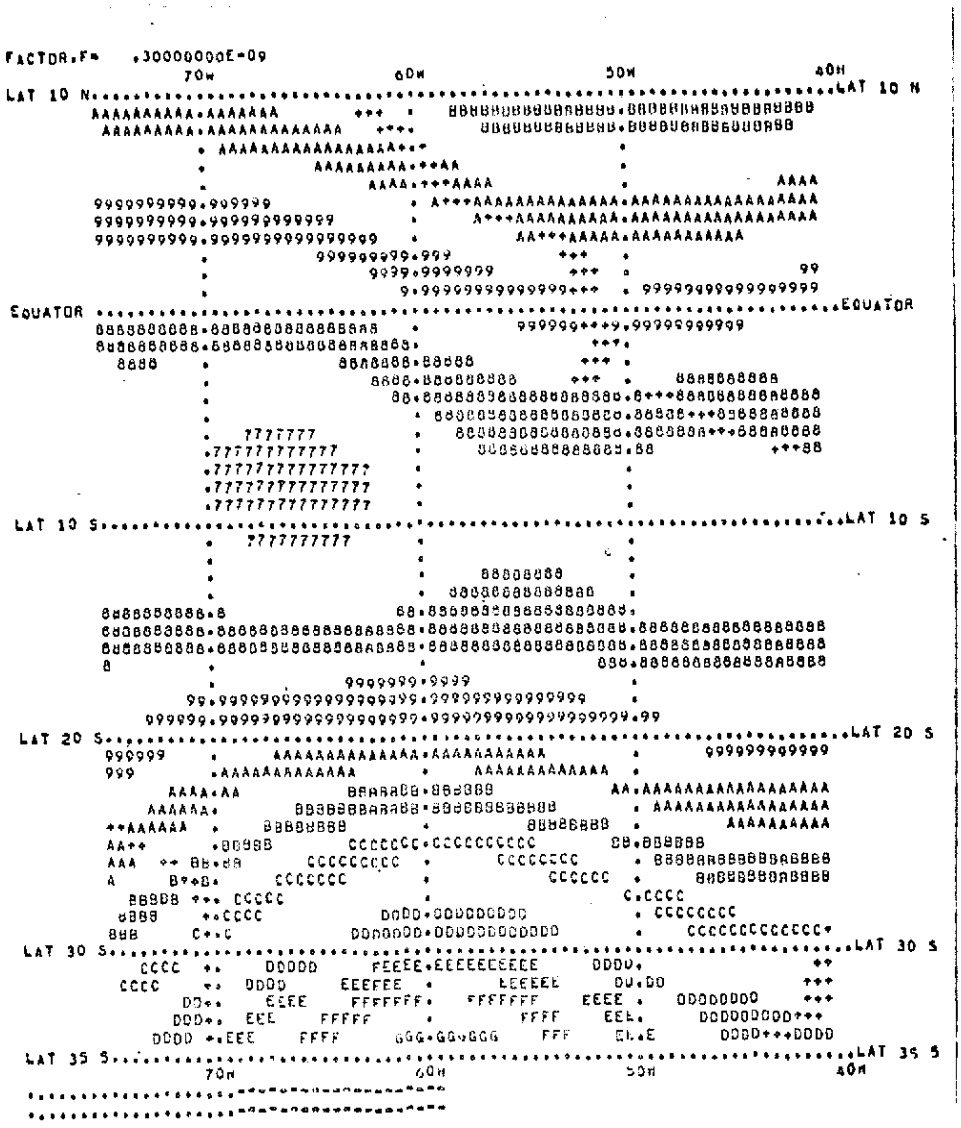

Fig. 5 (A) - ψ for 12/10/71 1200 GMT; 300 mb, observed (t = 0 h)

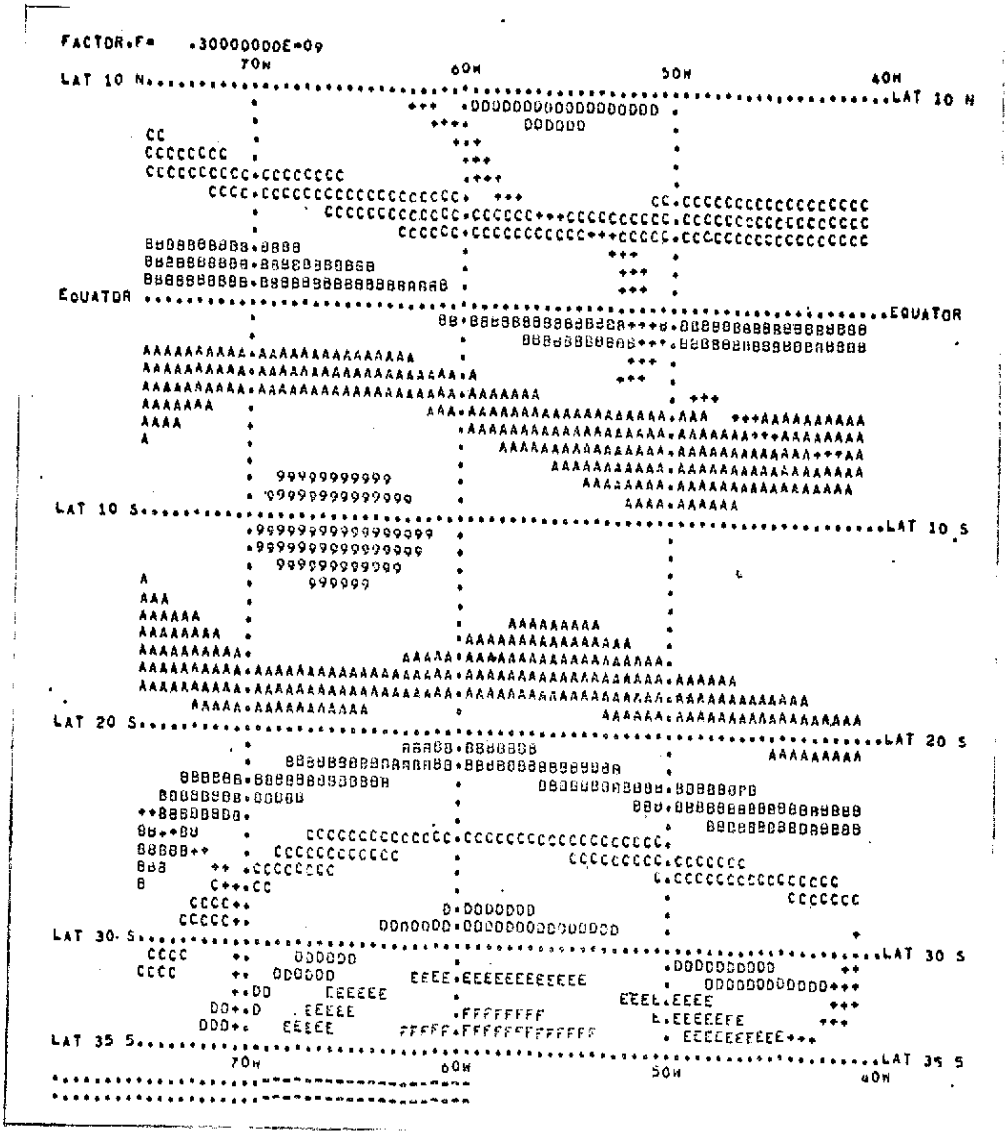

Fig. 5 (B) - ψ for 12/10/71 1200 GMT; 500 mb, observed (t = 0 h)

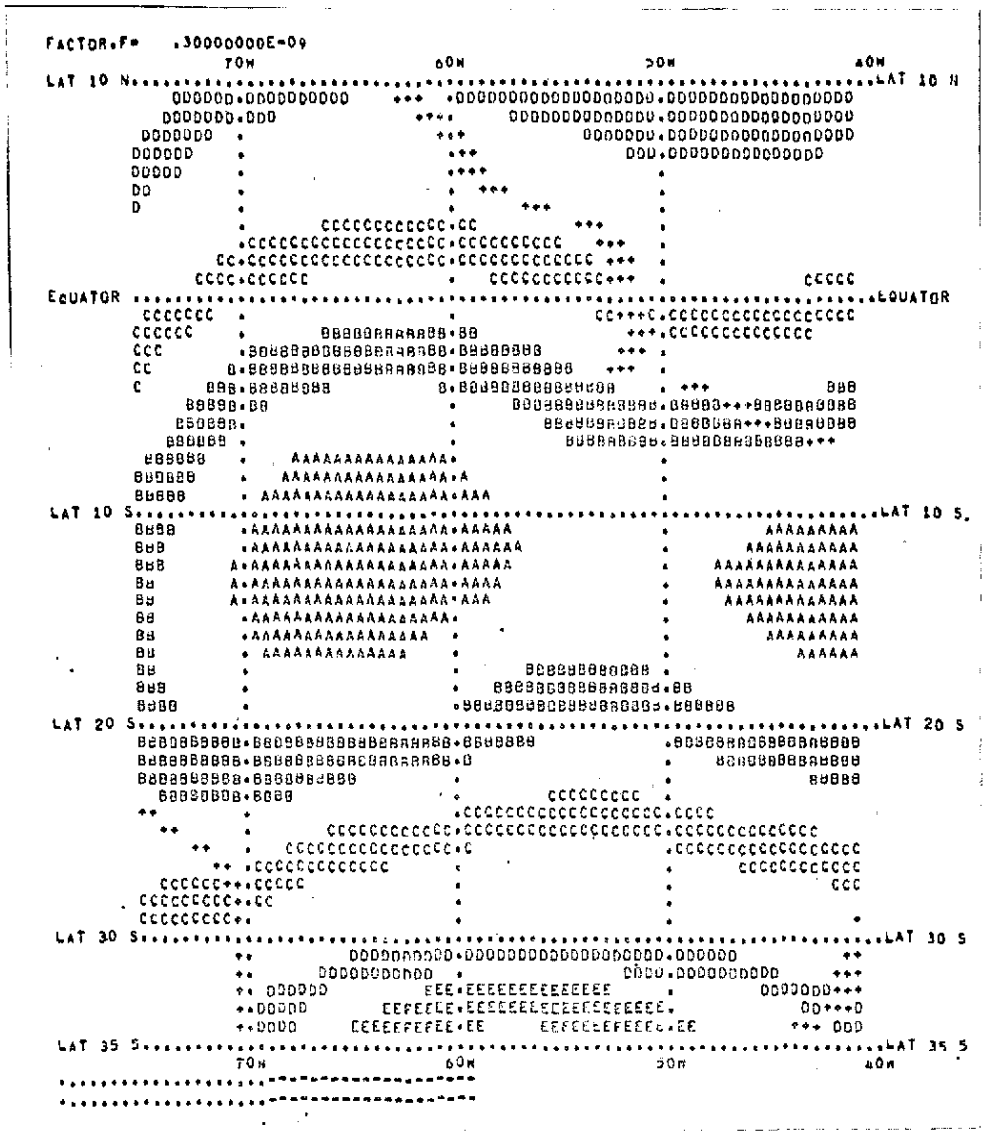

Fig. 5 (C) - ψ for 12/10/71 1200 GMT; 700 mb, observed (t = 0 h)

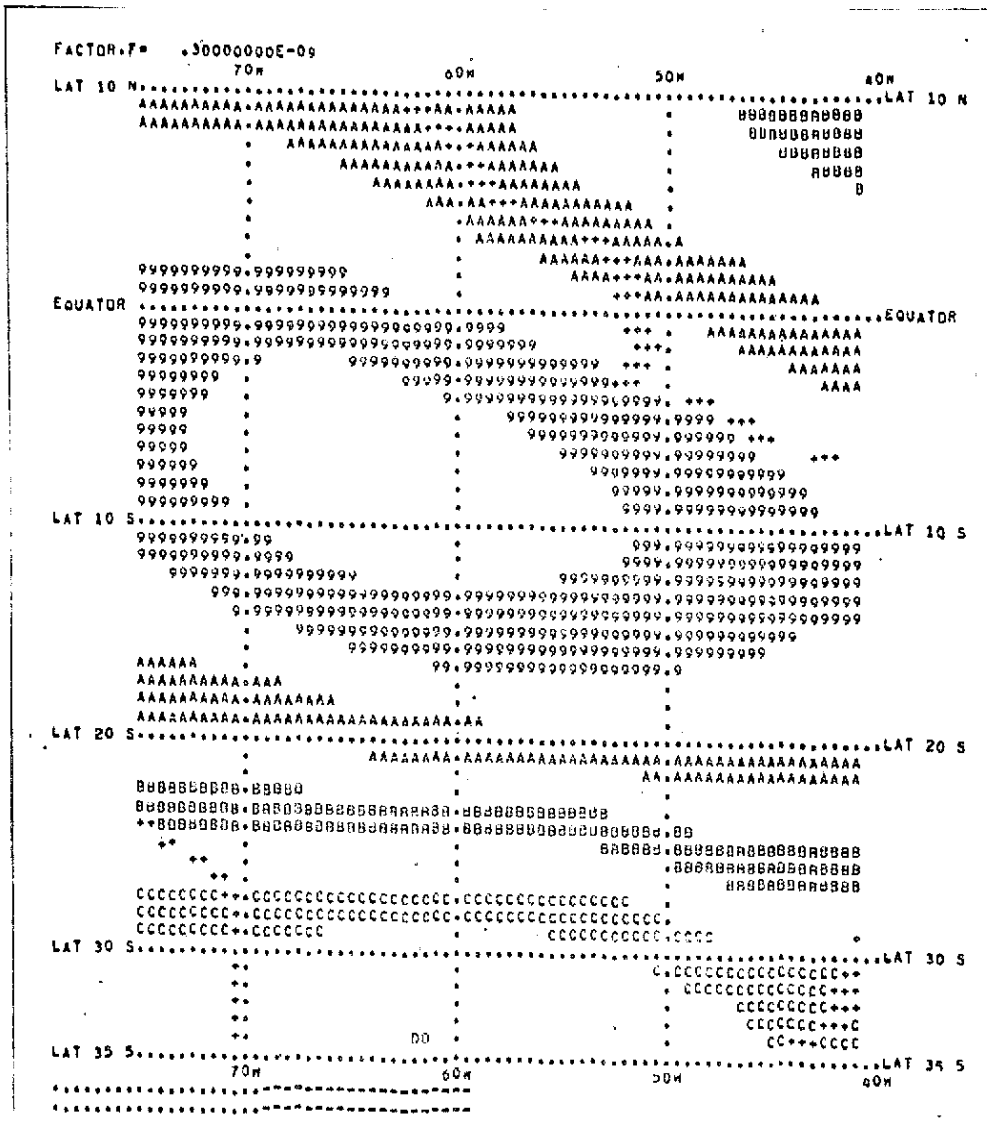

Fig. 5 (D) - Forecast ψ for 13/10/71 1200 GMT; 300 mb (t = 24 h)

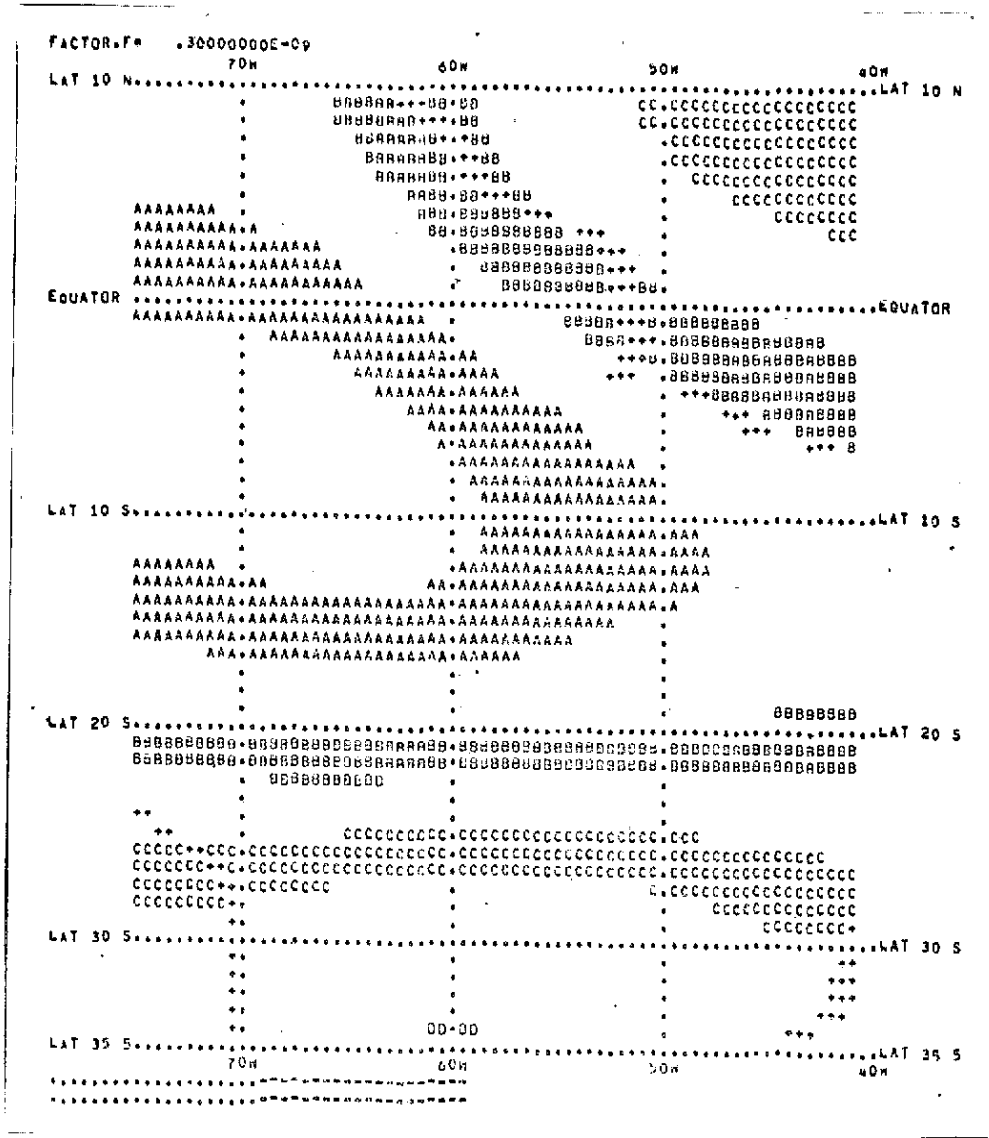

Fig. 5 (E) - Forecast ψ for 13/10/71 1200 GMT; 500 mb (t = 24 h)

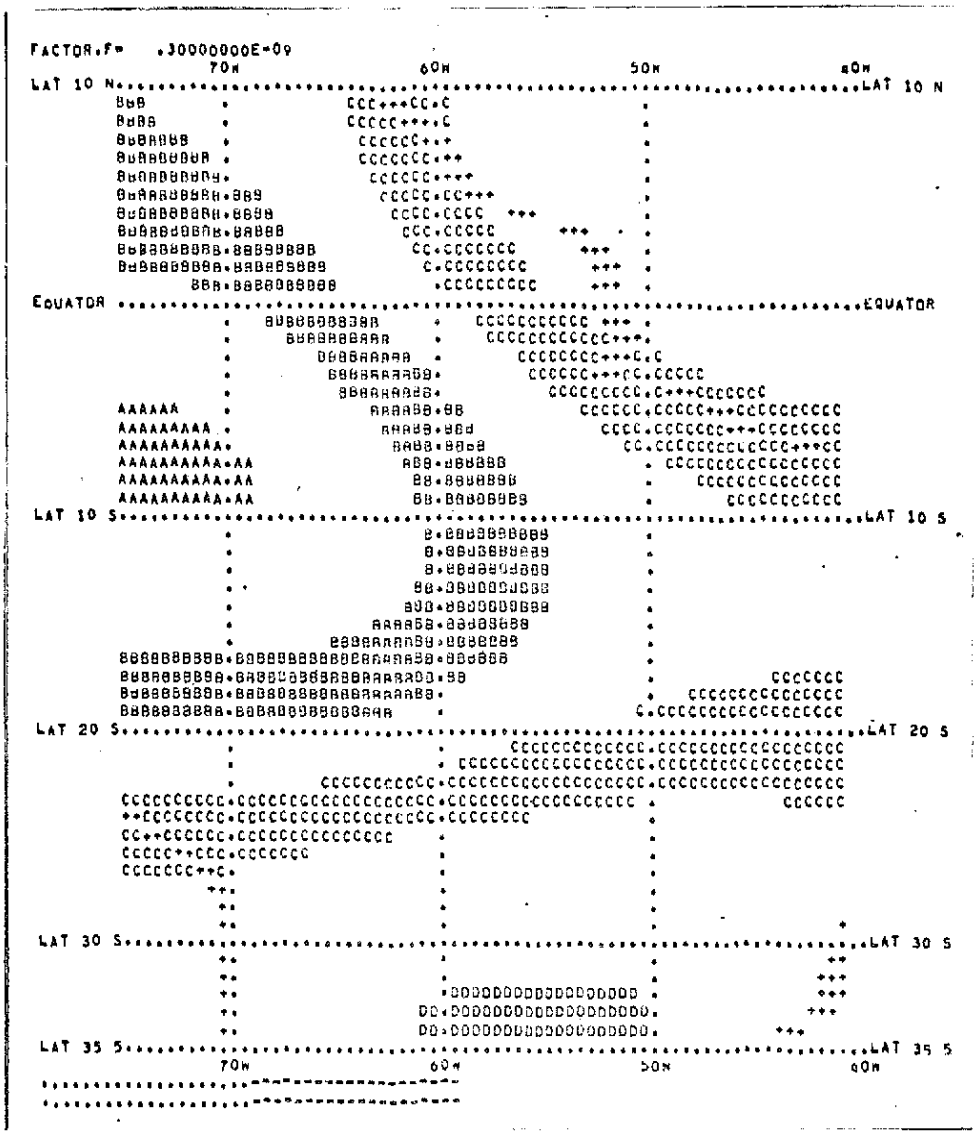

Fig. 5 (F) - Forecast ψ for 13/10/71 1200 GMT; 700 mb (t = 24 h)

Fig. 5 (G) - (Observed) ψ for 13/10/71 1200 GMT; 300 mb (t = 24 h)

Fig. 5 (H) - (Observed) ψ for 13/10/71 1200 GMT; 500 mb (t = 24 h)

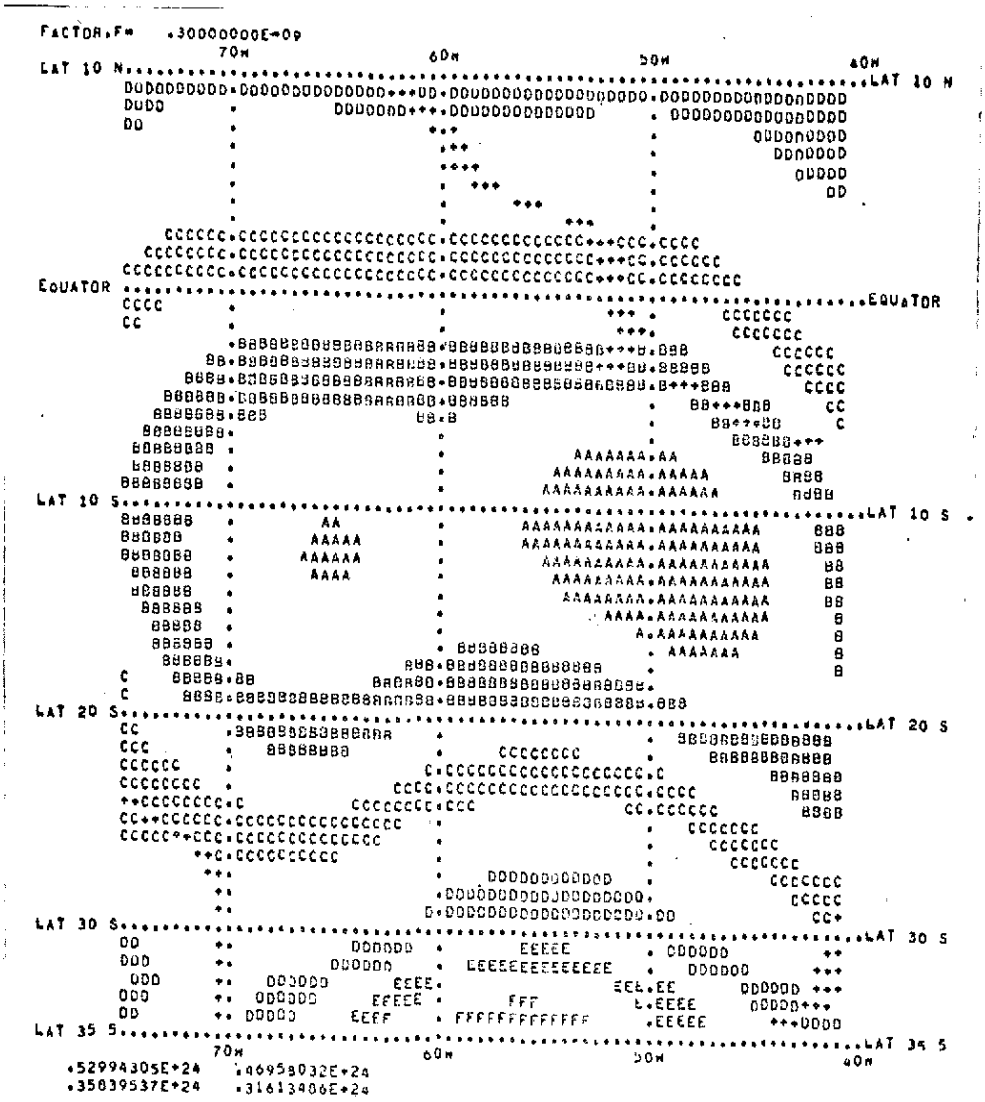

Fig. 5 (I) - (Observed) ψ for 13/10/71 1200 GMT; 700 mb (t = 24h)

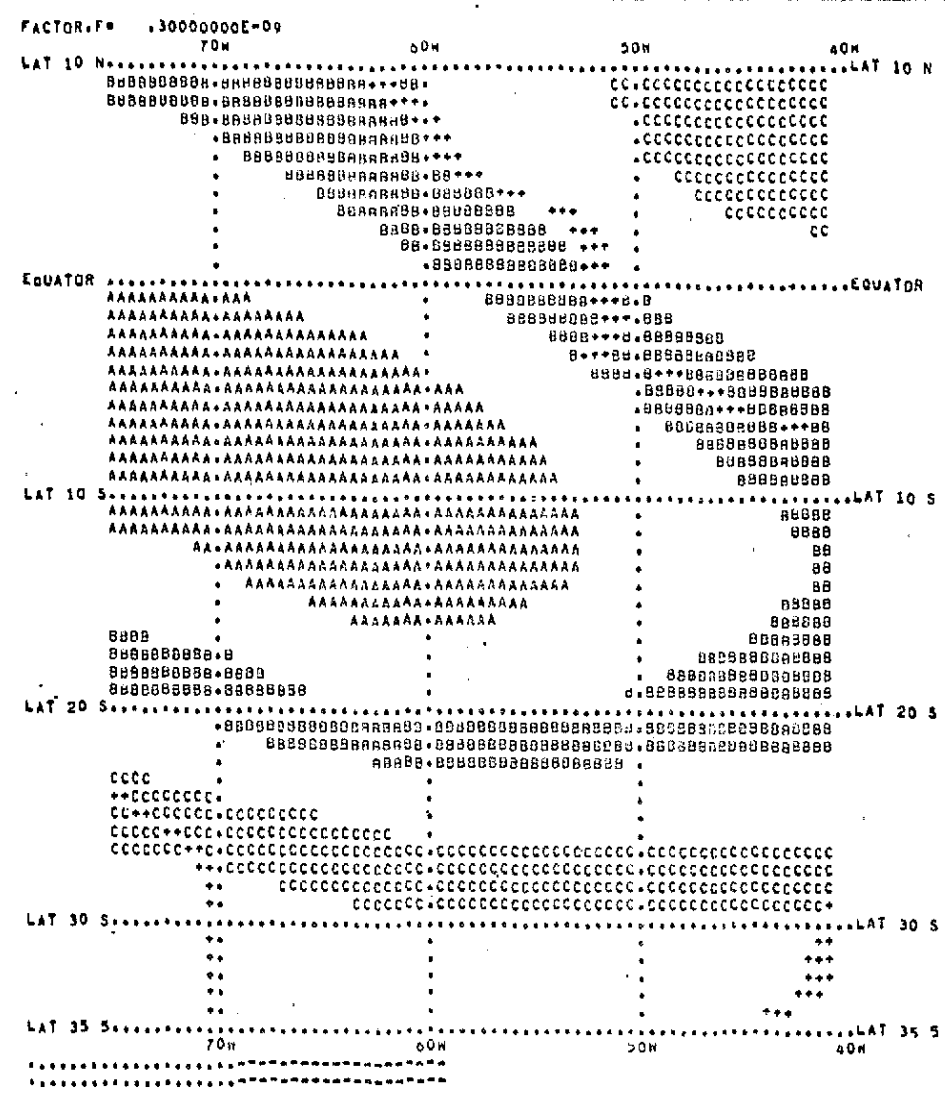

Fig. 6 (A) - Forecast ψ for 14/10/71 1200 GMT; 300 mb (t = 48 h)

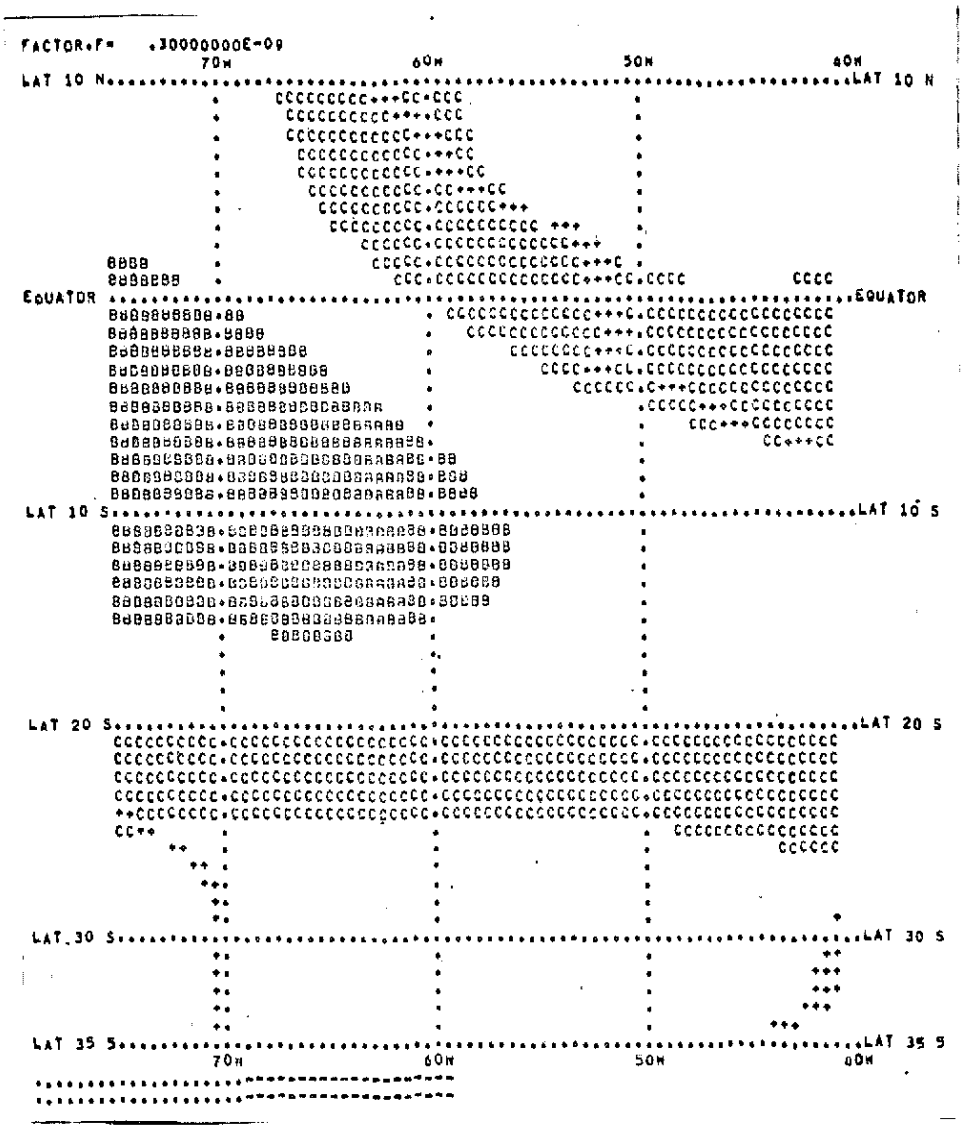

Fig. 6 (B) - Forecast ψ for 14/10/71 1200 GMT; 500 mb (t = 48 h)

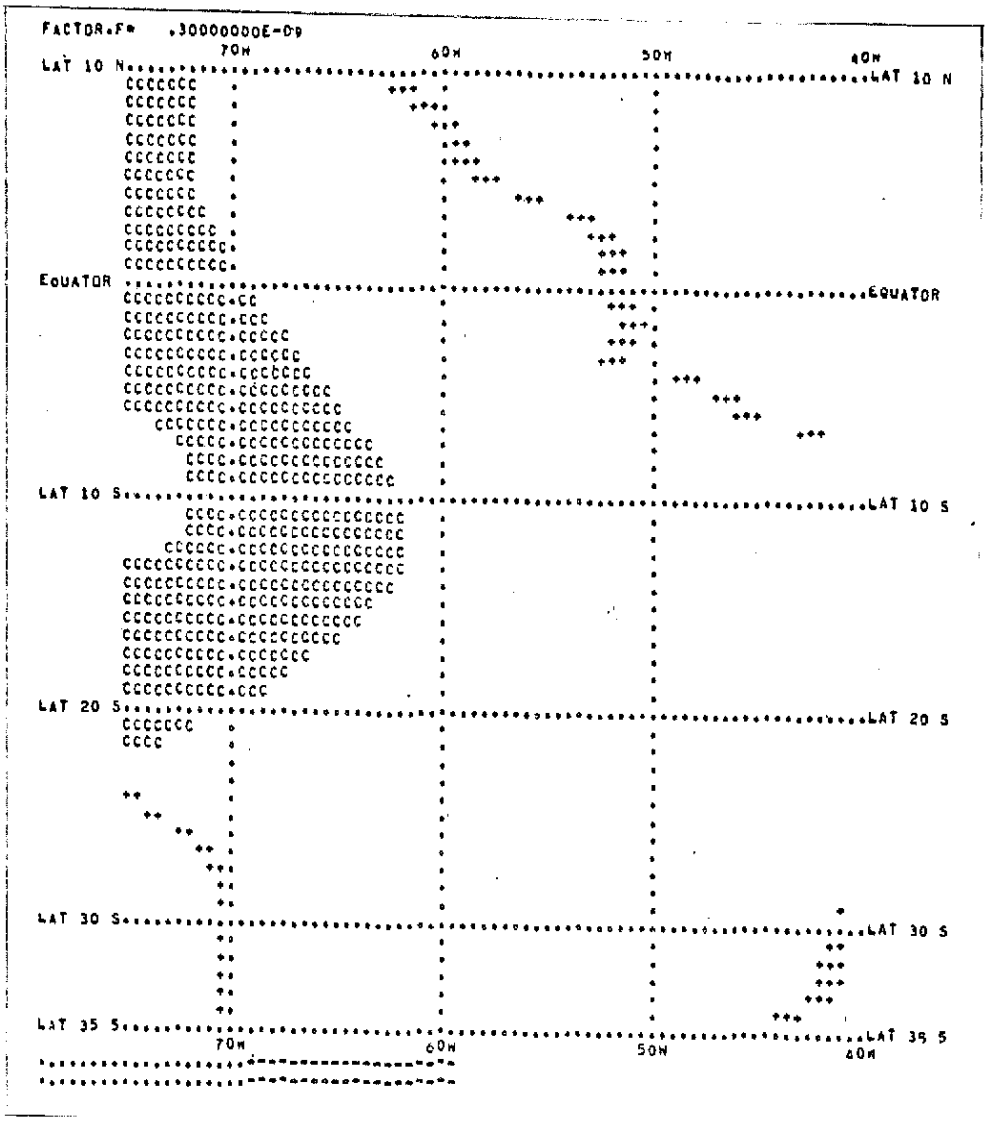

Fig. 6 (C) - Forecast ψ for 14/10/71 1200 GMT; 700 mb (t = 48 h)

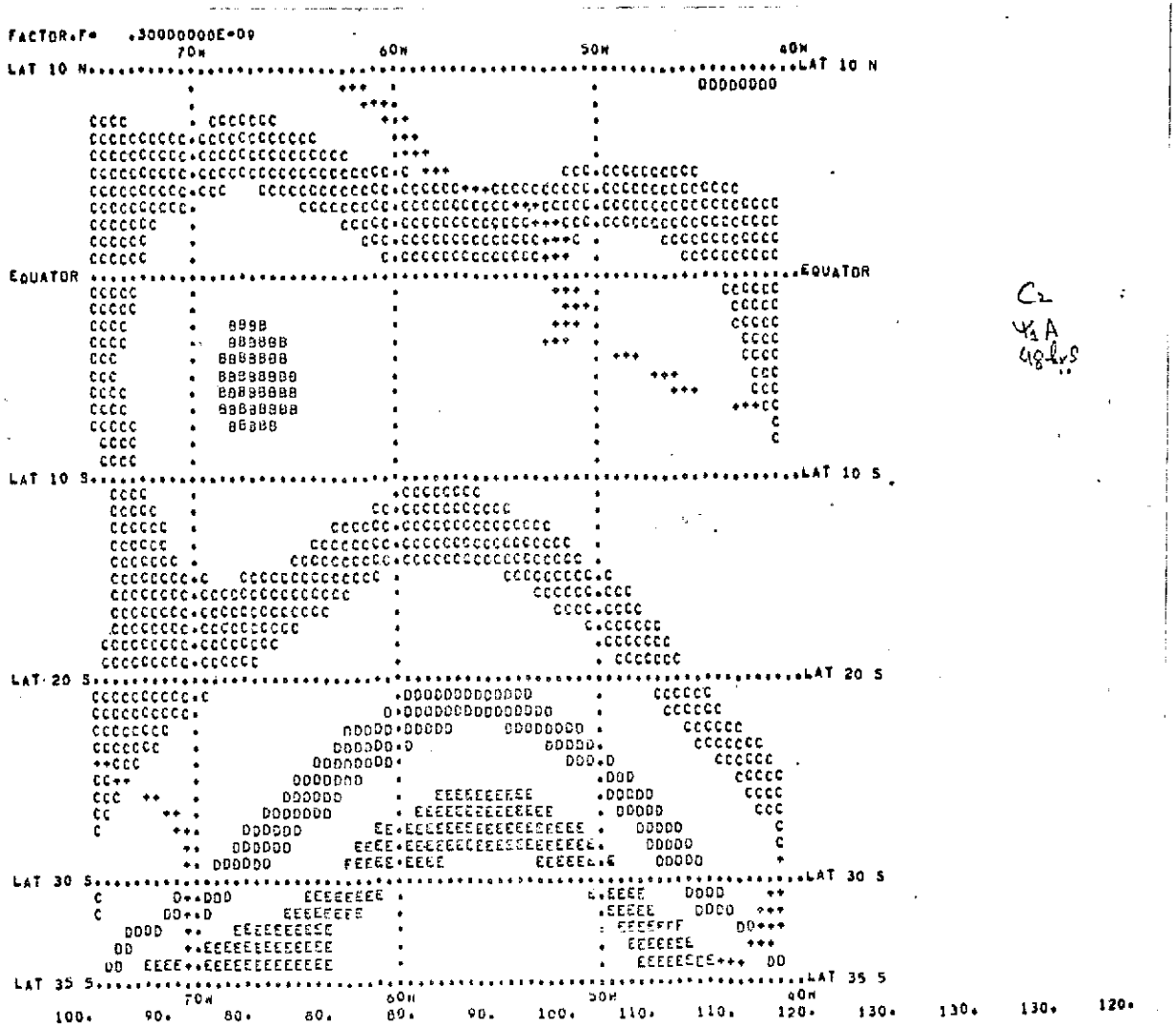

Fig. 6 (D) - (Observed) ψ for 14/10/71 1200 GMT; 300 mb (t = 48 h)

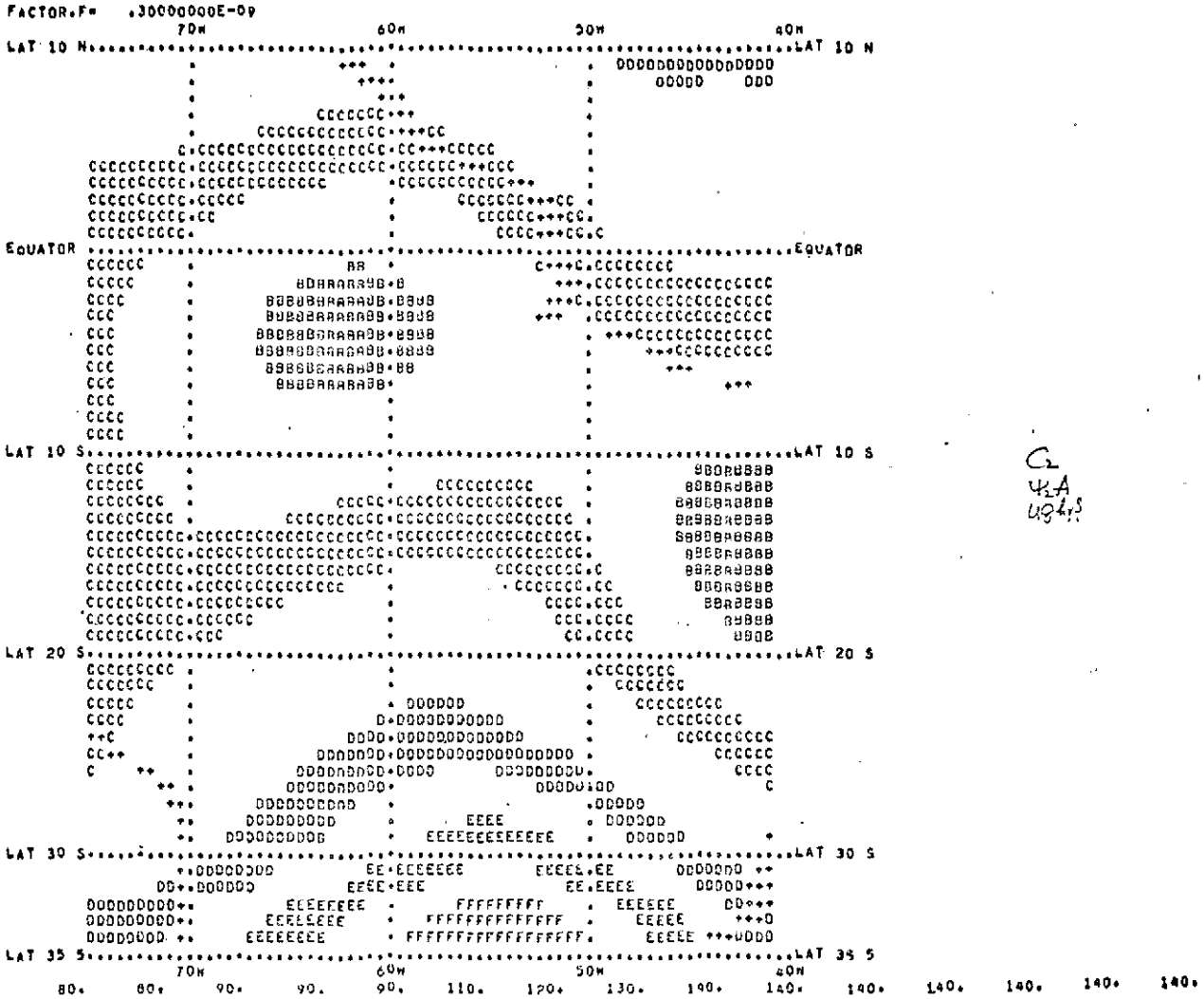

Fig. 6 (E) - (observed) ψ for 14/10/71 1200 GMT;
500 mb (t = 48 h)

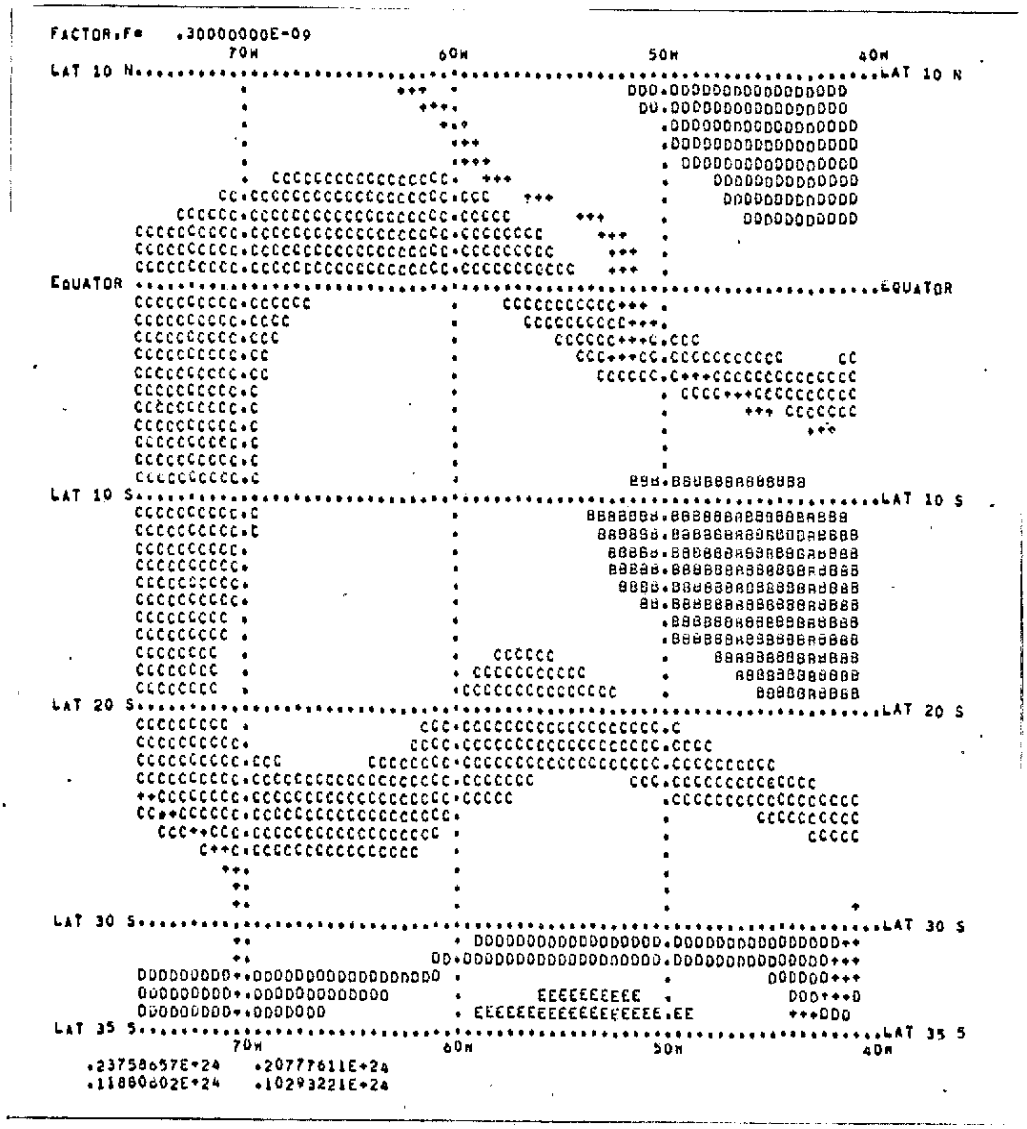

Fig. 6 (F) - (Observed) ψ 14/10/71 1200 GMT; 700 mb (t = 48 h).

TABLE 1

ABSTRACT OF NUMERICAL COMPARISON OF WINDS OBSERVED AND FORECAST FOR T = 24 H FOR THE 09/08/71 CASE

LAT.	Nº	R	ρ_1	LONG.	Nº	ρ_2
			300 mb			
35°S	1	7.5	.91			
25°S	5	14.6	.70	70	1	.90
15°S	9	6.9	.30	60	5	.96
5°S	13	6.3	.15	50	9	.86
5°N	17	7.1	-.77	40	13	.49
			500 mb			
35°S	1	4.1	.64			
25°S	5	5.5	.88	70	1	.84
15°S	9	5.9	.85	60	5	.92
5°S	13	1.5	.11	50	9	.82
5°N	17	2.0	.70	40	13	.78
			700 mb			
35°S	1	3.9	-.12			
25°S	5	4.1	.78	70	1	.80
15°S	9	7.9	.54	60	5	.89
5°S	13	5.3	-.74	50	9	.92
5°N	17	4.9	-.19	40	13	.92

R: Root mean-square derivation of wind-speed.

ρ_1: Correlation coefficient between forecast wind actual meridional components of winds

ρ_2: Correlation coefficient between forecast and actual zonal component of wind.

TABLE 2

ABSTRACT OF NUMERICAL COMPARISON OF WINDS OBSERVED AND FORECAST FOR T = 24 H FOR THE 12/10/71 CASE

300 mb

LAT.	Nº	R	ρ_1	LONG.	Nº	ρ_2
35°S	1	4.6	.88			
25°S	5	24.7	-.63	70	1	.97
15°S	9	2.9	.44	60	5	.96
5°S	13	2.8	.79	50	9	.93
5°N	17	4.0	.59	40	13	.92

500 mb

35°S	1	3.2	.90			
25°S	5	4.9	.96	70	1	.95
15°S	9	5.1	.74	60	5	.97
5°S	13	3.8	-.46	50	9	.91
5°N	17	3.4	.26	40	13	.97

700 mb

35°S	1	6.3	-.01			
25°S	5	4.9	-.05	70	1	.68
15°S	9	3.2	-.27	60	5	.77
5°S	13	2.1	-.70	50	9	.85
5°N	17	3.2	.38	40	13	.86

TABLE 3

ABSTRACT OF NUMERICAL COMPARISON OF WINDS OBSERVED AND FORECAST FOR T = 48 H FOR THE 12/10/71 CASE

300 mb

LAT.	Nº	R	ρ_1	LONG.	Nº	ρ_2
35°S	1	4.4	.50			
25°S	5	8.7	.84	70	1	.80
15°S	9	8.7	.72	60	5	.83
5°S	13	3.9	-.30	50	9	.88
5°N	17	2.7	.17	40	13	.70

500 mb

35°S	1	4.6	.19			
25°S	5	4.2	.93	70	1	.87
15°S	9	3.7	-.13	60	5	.71
5°S	13	3.3	.42	50	9	.66
5°N	17	2.7	-.34	40	13	.92

700 mb

35°S	1	3.4	-.30			
25°S	5	2.9	.47	70	1	.15
15°S	9	3.6	-.14	60	5	.25
5°S	13	5.0	.78	50	9	.61
5°N	17	5.2	-.47	40	13	.88